FABRICATION AND CHARACTERIZATION OF NANOSTRUCTURED LIPID CARRIERS LOADED WITH MANGIFERIN TO IMPROVE ITS THERAPEUTIC POTENTIAL

THESIS SUBMITTED IN PARTIAL FULFILLMENT FOR THE
REQUIREMENTS OF THE DEGREE OF
MASTER OF PHARMACY

SUBMITTED BY
MR. HIRANMOY BHATTACHARYA
ROLL NUMBER- 002011402024
REGISTRATION NUMBER- 136648 OF 2016-2017
EXAMINATION ROLL NUMBER- M4PHG22002

UNDER THE GUIDANCE OF
PROF. SAIKAT DEWANJEE

DEPARTMENT OF PHARMACEUTICAL TECHNOLOGY
FACULTY OF ENGINEERING AND TECHNOLOGY
JADAVPUR UNIVERSITY
KOLKATA 700032, INDIA
2022

Certificate of Approval

This is to certify that thesis entitled "**Fabrication and Characterization of Nanostructured Lipid Carriers Loaded with Mangiferin to Improve Its Therapeutic Potential**" has been carried out by **Mr. Hiranmoy Bhattacharya** under the supervision of Prof. Saikat Dewanjee, Department of Pharmaceutical Technology, Jadavpur University, Kolkata 700032. He has incorporated her findings into this thesis of the same title, being submitted by her, in partial fulfillment of the requirements for the degree of "Master of Pharmacy" of this university. He has pursued this work independently with proper attention to my entire satisfaction.

Supervised by

PROF. SAIKAT DEWANJEE
Project supervisor
Advanced Pharmacognosy Research Laboratory
Department of Pharmaceutical Technology
Faculty of Engineering and Technology
Jadavpur University
Kolkata 700032, India

PROF. SANMOY KARMAKAR
Head
Department of Pharmaceutical Technology
Faculty of Engineering and Technology
Jadavpur University
Kolkata 700032, India

PROF. CHANDAN MAZUMDAR
Dean
Faculty of Engineering and Technology
Jadavpur University
Kolkata 700032, India

DECLARATION

I, the undersigned solemnly declare that the project report on "**Fabrication and Characterization of Nanostructured Lipid Carriers Loaded with Mangiferin to Improve Its Therapeutic Potential**" is submitted in the partial fulfillment of the degree of "Master of Pharmacy", under the supervision of Prof. Saikat Dewanjee, Department of Pharmaceutical Technology, Jadavpur University, Kolkata 700032. I assert the statements made and conclusions drawn are an outcome of my research work. I further certify that the work contained in the report is original and has been done by me under the general supervision of my supervisor.

Mr. Hiranmoy Bhattacharya

Roll No. 002011402024

Registration No. 136648 of 2016-2017

Examination Roll No. M4PHG22002

ACKNOWLEDGEMENTS

*It gives me a great pleasure to acknowledge my immense respect and depth of gratitude to my guide **Prof. Saikat Dewanjee**, Advanced Pharmacognosy Research Laboratory, Department of Pharmaceutical Technology, Jadavpur University; who has been a constant source of encouragement and treasure of valuable inspiring guidance without which this project work would never been possible.*

*I express my sincere gratitude to **Prof. Sanmoy Karmakar**, Head, Department of Pharmaceutical Technology, Jadavpur University for providing me with necessary facilities to carry out my project work.*

*I would love to take this opportunity to thank my seniors, especially **Mr. Pratik Chakraborty**, as well as **Dr. Swarnalata Joarder**, **Mr. Avigyan Saha**, **Mr. Rakesh Karmakar, Ms. Udita Paul, Mr. Rounak Ram** and **Mrs. Chandrima Sarkar** who have helped me tremendously to conduct my research work and devising my thesis. I would also like to thank my juniors **Mr. Chiranjib Bhattacharyya** and **Mrs. Shrestha Bhanja** for their help and encouragement.*

*I also express my thanks to all my friends of Department of Pharmaceutical Technology, Jadavpur University, especially to **Mr. Abhishek Kumar**, **Mr. Subhankar Saha**, **Mr. Sandipan Mallick** and **Mr. Rajorshi Das** for being unselfishly there for me.*

*Finally, I express my love and gratitude to all of my family members and relatives for giving me the strength and support to reach to this destination. I would also like to thank my special friend **Ms. Koyel Roy** for her continuing support in this journey.*

Date: *(**Hiranmoy Bhattacharya**)*

Place:

DEDICATED TO MY PARENTS

MR. MIHIR BHATTACHARYA AND MRS. SOMA BHATTACHARYA

CONTENTS

FIGURE CAPTIONS

TABLE CAPTIONS

PREFACE

Many naturally occurring small molecules possess several therapeutic attributes, such as anti-diabetic, anti-hyperlipidemic, antioxidant, immunomodulatory, anti-allergic activities, etc.; however, simultaneously exhibit poor pharmacokinetic and biopharmaceutical attributes; which largely restrict their therapeutic effects. To overcome the pharmaceutical problems associated with these molecules and to enhance the therapeutic efficacy, several novel drug delivery strategies have been developed. A unique blend of various branches of science, such as polymer technology, pharmaceutics, immunology, molecular biology, nanotechnology, etc. have integrally contributed in designing various novel delivery platforms of therapeutic drugs. A growing body of evidence shows that nanotechnology has gained extensive attention to the different research area due to their variety of applications. Therapeutic nanoparticles are the main interest in medicinal field, to fulfill the criteria of novel drug delivery systems to improve bioavailability and achieve site-specific action among many others. Over the years, researchers have proposed different physicochemical methods to develop versatile nanoplatforms for the delivery of therapeutic agents to achieve desired effects. Mangiferin is one of the naturally occurring polyphenols having similar biopharmaceutical and pharmacokinetic challenges. Thus, it has been aimed to formulate mangiferin-loaded nanostructured lipid carriers to enhance the bioavailability of mangiferin to achieve better therapeutic response.

This thesis has been divided into six different chapters. Chapter 1 describes a brief introduction to the fundamentals and advantages of nanoformulation in drug delivery, chapter 2 contains contextual literature survey, chapter 3 expresses the aims and objectives of the current study, chapter 4 comprises materials and methods used to execute the research, chapter 5 deals with the results and relevant discussions, and chapter 6 demonstrates the conclusion of the study.

Chapter 1

Introduction

Contents

1. Introduction

Nanoscience and nanotechnology refer to structures, technologies, and systems that have novel features and functionalities as a result of the arrangement of their atoms on the nanometre (nm) scale (Bayda et al., 2019). The prefix 'nano' refers to a Greek prefix that means 'dwarf' or ‘very little' and represents a thousand millionth of a metre (Bayda et al., 2019). Humans first employed nanoparticles (NPs) and structures in the fourth century AD, when the Romans exhibited one of the most fascinating examples of nanotechnology in the ancient world (Bayda et al., 2019). The first scientific description of NPs preparation is marked by Faraday way back in 1857 (Edwards and Thomas, 2007). Because of their wide range of applications, NPs and nanotechnology have received a lot of attention in various scientific fields since then. Therapeutic NPs are still a hot topic in medicine, as they can meet the criterion of novel drug delivery systems (NDDS) such as appropriate bioavailability and site-specific activity, among other things. Researchers have developed a number of physicochemical ways for framing various types of synthetic NPs that can be used to create a well-defined nanocarrier system. Due to the poisonous and harmful nature of NPs, further research into biological or environmentally benign approaches to circumvent the constraints is needed.

Mangiferin (Mgn), (2-β-D-glucopyranosyl-1,3,6,7-tetrahydroxy-9H-xanthen-9-one) is a naturally occurring polyphenolic compound which has several therapeutic uses. Mgn is obtained from different parts of the plants *Mangifera indica, Iris unguicularis, Cyclopia sp* (Khurana et al., 2016). The therapeutic effects of Mgn extend to anti-cancer effect by inhibiting the initiation, progression and metastasis of cancer, anti-inflammatory effect by targeting and modulating various pro-inflammatory signaling intermediates, anti-oxidant and free-radical scavenging effect due to our hydroxyl groups in its structure, anti-diabetic effect by decreasing insulin resistance etc (Rajendran et al., 2014; Saha et al., 2016; Imran et al., 2017; Zhang et al., 2019). However, Mgn has very poor solubility and membrane permeability, which leads to poor bioavailability (Mei et al., 2021). This results in less available Mgn in the target site to deplete its therapeutic value of it, hence a compatible formulation which will improve bioavailability is required. Herein Mgn loaded nanostructured lipid careers (Mgn-NLCs) using polyvinyl alcohol (PVA) as an emulsifier by emulsion-solvent evaporation technique has been reported. Characterization by means of particle size, surface morphology, surface charge, physicochemical characteristics, drug encapsulation efficiency and *in vitro* release profile has been undertaken for evaluation.

1.1. Advantages of nanoscale formulations

Nanocarrier-based drug delivery offers several advantages in the field of medicine which are detailed below.

1.1.1. Enhanced solubility and dissolution rate of drug

Because of their small dimensions, NPs have a large effective surface area, resulting in a high concentration gradient of poorly soluble molecules, regulated pharmacokinetic features, and a faster dissolution rate of the contained pharmaceutical component (Dibaei et al., 2019). Due to the particle size, NPs containing both hydrophobic and hydrophilic drugs become highly soluble (Hogarth et al., 2021). When hydrophobic drugs that are less bioavailable are included in NPs, they can attain a higher degree of bioavailability than when used in conventional drug delivery methods. (Hogarth et al., 2021).

1.1.2. Increased bioavailability

As NPs have a higher solubility in the systemic circulation than free drugs, they provide greater systemic exposure and a faster peak plasma concentration than other standard oral formulations, with a shorter median time to maximum drug concentration (Din et al., 2017). NPs can also boost the oral bioavailability of both hydrophobic and hydrophilic drugs, according to research (Wang et al., 2020). Since NPs are biodegradable, they release the drug over a lengthy period of time, resulting in improved bioavailability (Su and Kang, 2020).

1.1.3. Long duration of action

NPs contribute to interactions with targeted tissues and cells, which allows for enhanced lipid-lipid exchange with NPs' lipid monolayer (Tenchov et al., 2021). This characteristic of NPs makes them good drug repositories, as they have slow-release kinetics and stay at the target site for a long time (Patra et al., 2018).

1.1.4. Targeted drug delivery

NPs offer targeted drug delivery to organs, tissues, and cells while also reducing toxicity (Patra et al., 2018). It could be an active or passive targeted delivery method. The therapeutic drug is coupled to a tissue or cell-specific ligand in active targeting (Yoo et al., 2019). The therapeutic agent is incorporated into NPs that are passively delivered to the target organ in passive targeting (Attia et al., 2019). Furthermore, as it can cross the blood-brain barrier, drug-loaded NPs are a safe and effective technique to get pharmaceuticals into the central nervous system (Dong, 2018).

1.2. Classification of NPs

NPs intended for drug delivery, diagnostic and other clinical uses are of various types (Figure 1.1) based on their structure and different purposes; these include nanomicelle, carbon nanotubes, metallic NPs, polymeric NPs, mesoporous silica NPs, lipid-based NPs etc.

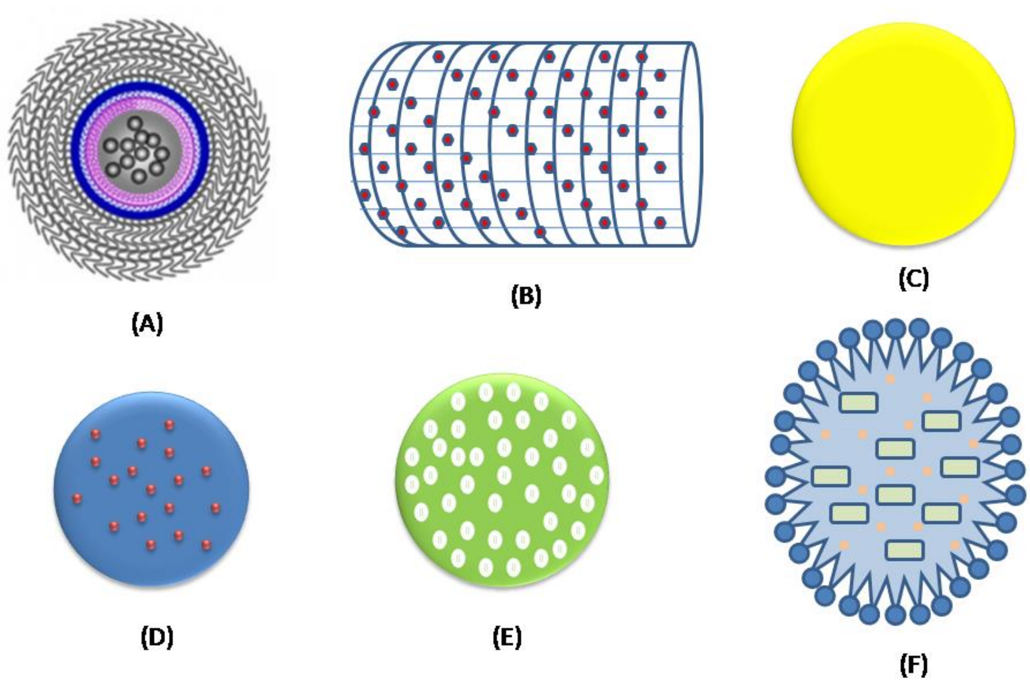

Figure 1.1. Different types of NPs. Nanomicelles (A), carbon nanotubes (B), metallic NPs (C), polymeric NPs (D), mesoporous silica NPs (E), and lipid NPs (F).

1.2.1. Nanomicelles

The first nanomicelles were created in 1984. The polymers used to create nano-micelles must degrade naturally. Numerous polymers are widely used to create nanomicelles, including poly(lactide), poly(propylene oxide), poly(glycolide), poly(lactide-co-glycolide), and poly(-caprolactone), with polyethylene glycol being the most often used hydrophilic polymer. Nano-micelle research is advancing and encouraging the field of drug delivery for the solubilization, stability, and distribution of specific pharmaceuticals. The unique quality of polymeric micelles is their ability to encapsulate hydrophobic drugs in the core while allowing the exterior to be modified appropriately (Mallya et al., 2020).

1.2.2. Carbon nanotubes

Carbon nanotubes (CNTs) have attracted a lot of attention among various carbon-based nanocarriers (fullerenes, carbon nanotubes, graphene, cones, etc.) and spherical NPs because of their distinctive properties, including ultra-high aspect ratio, high cargo loading, and intracellular bioavailability. Since CNTs are lipophilic, which causes cellular buildup and toxicity, they have been functionalized (f-CNT) to overcome this intrinsic drawback and increase their solubility and biocompatibility (Kiran et al., 2020).

1.2.3. Metallic NPs

Novel metals have been used to develop nanoformulations due to their fewer chemical reactivities. Au NPs, or gold NPs, are efficient radiosensitizers used in cancer therapy and drug administration, among other medical procedures. Recent developments in nanomaterial synthesis and production technologies have made it possible for precise technology to readily regulate particle factors like size, composition, shape, and surface chemistry. The NPs surface can also be coated with a biocompatible surface layer to offer stabilization under physiological conditions. These NPs can be used as contrast agents in multimodal imaging, drug delivery carriers, and cancer therapy enhancers (Siddique and Chow, 2020). Silver, another noble metal is also used for the formulation of NPs. Small compounds, such as antisense oligonucleotides, and other medicinal substances have been delivered by silver NPs. Due to its antibacterial, antiviral, antifungal, and antioxidant properties as well as its unusually enhanced physicochemical properties compared to the bulk material, such as optical, thermal, electrical, and catalytic properties, silver is the most commercially viable precious metal used in the preparation of NPs and nanomaterials. Small silver NPs have many benefits as drug delivery systems, including controllable size and shape, improved surface-bound nucleic acid stability, high-density surface ligand attachment, transmembrane delivery without harsh transfection agents, protection of the attached therapeutics from deterioration, and the potential for improved timed/controlled intracellular drug delivery. Due to its low cost, ability to create a healthier workplace, and protection of human health, plant-mediated synthesis of silver NPs is gaining popularity. This will result in less waste and safer products (Ivanova et al., 2018). Along with noble metals, iron oxides are used in formulating NPs for drug delivery owing to their magnetic properties. Due to their combination of hollow architectures, magnetic iron oxide NPs have shown significant potential as distinctive carriers in the delivery of drugs. Importantly, magnetic materials are ubiquitous tools for the magnetic separation of tiny molecules, biomolecules, and cells because of their combination of responsiveness to an external magnetic field and the expansive possibilities of their coatings (Mohammadi et al., 2019).

1.2.4. Polymeric NPs

Macromolecules known as polymers are created by the covalent joining of one or more types of units, known as monomers, to form a straight or branching chain. As long as they have at least two functional groups where they can interact with another monomer, these monomers can have any structure. Ideally, a polymer may be created to have particular qualities by choosing the appropriate monomer or monomers. They can be tailored to fit the needs or end goals owing to the exceptional synthetic versatility they provide. These are the causes behind the increasing importance of polymeric materials in nanotechnology generally and their application as NPs precursors for drug delivery systems (Begines et al., 2020). One of the most studied subjects today is polymeric NPs. Their main benefits include enhanced treatment efficacy, longer clearance times, good size management, and lower toxicity. Dendrimers, ligand-based NPs, polymeric micelles, PEGylated NPs, etc. are a few examples of the many types of polymer-based NPs (Sur et al., 2019).

1.2.5. Silica NPs

This new class of materials is characterised by an ordered distribution of pores with homogeneous sizes ranging from 2 to 20 nm, high pore volume (approximately 1 cm^3/g), large surface area (approximately 1000 m^2/g), and a high density of silanol groups at their surface, which may facilitate subsequent functionalization processes. MSMs were the perfect choice for applications like drug delivery systems that can call for the adsorption of molecules because of these characteristics. The development of novel, cutting-edge multifunctional materials for a wide range of biotechnological applications has been sparked by the MSNs' exceptional qualities for biomedical applications. The most recent advances in biological research employing MSNs may serve as some of the pillars for highly selective, tailored therapies and diagnostic procedures in the future. In this way, the development of NPs capable of establishing close relationships with the biological world is made feasible by the ongoing breakthroughs in nanotechnology, including synthesis and characterization techniques (Manzano and Vallet-Regí, 2020).

1.2.6. Lipid-based NPs

1.2.6.1. Liposomes

The spherical vesicles known as liposomes have an aqueous core inside one or more concentric phospholipid bilayers. Liposomes are an effective medication delivery mechanism for many pharmaceuticals since they are harmless and biodegradable. By stabilizing substances, removing barriers to cellular and tissue absorption, enhancing medication biodistribution to target areas in vivo, and lowering systemic toxicity, they have increased the therapeutic efficacy of pharmaceuticals (Guimarães et al., 2021). Liposomes are the most researched lipid-based nanocarriers and have exceptional biocompatibility and biodegradability. Despite being widely used in drug delivery applications, they have chemical and physical stability concerns that could lead to particle aggregation and drug deterioration during storage (Nakhaei et al., 2021). As a result, novel lipid medicine delivery techniques have been developed.

1.2.6.2. Solid lipid NPs

Solid lipid NPs (SLNs) were suggested as a possible solution to the issues with liposomes mentioned above. They can be created from a range of lipids, including waxes and triglycerides like cetyl palmitate and beeswax that are solid at both body and room temperatures, fatty acids, and triglycerides with various chain lengths (Ahmad and Ahsan, 2020). Surfactants also play a crucial role in the creation of SLNs because of their ability to accumulate at the binding interface and lower the interfacial energy between the lipid and the aqueous phase. This helps the dispersion's physical stability. SLNs typically have a spherical shape with a diameter between 50 and 1000 nm. Lipids, which are solid at room temperature, emulsifiers, and occasionally a combination of both, as well as active pharmaceutical ingredients (APIs) and a suitable solvent system, are the main components of SLN formulations (Duan et al., 2020).

1.2.6.3. Nanostructured lipid careers

As the second generation of lipid NPs to address the drawbacks of the first generation, SLNs, nanostructured lipid carriers (NLCs) are emerging. The creation of NLCs involves the use of emulsifiers, solid and liquid lipids, and suitable biodegradable lipids. Incorporating liquid lipids (oil) results in structural flaws in solid lipids, resulting in a less ordered crystalline arrangement that prevents drug leakage and provides a high drug load. NLCs have drawn the attention of researchers in recent years as a potential replacement for SLNs, polymeric NPs, emulsions, microparticles, liposomes, etc. These nanocarriers can be used to deliver medications that are both lipophilic and hydrophilic. For the administration of medications via oral, parenteral, ophthalmic, pulmonary, topical, and transdermal routes, NLCs have emerged as a viable carrier system. Recently, NLCs have also been used in the administration of cosmeceuticals and nutraceuticals as well as chemotherapy, gene therapy, and brain targeting (Chauhan et al., 2020).

1.3. Biomedical application of NPs

The various processes have produced NPs that have been applied in a variety of sectors. Drug delivery, in vitro and in vivo diagnostics, nutraceuticals, and the creation of better biocompatible materials are some of the anticipated medical applications. NPs are mostly employed in the medical industry for drug delivery. Below are some of the current and potential uses of NPs in biology and medicine.

1.3.1. Drug delivery

There is growing hope that the application of nanotechnology to medicine may result in important improvements in illness diagnosis and treatment. Drugs with NPs contained in them either improve delivery to or uptake by target cells or lessen the toxicity of the free medication to organs other than the target ones (Mitchell et al., 2021). Conceptually, the delivery of medications has been transformed by nanotechnologies in general and NPs in particular. Today, the creation of NPs solutions containing medications has made it feasible to improve the activity and reduce the toxicity of numerous components while also increasing their therapeutic index. Thus, the change in size from tens of micrometres to tens or hundreds of nanometers has been a huge advancement in both technology and medicine (Jeevanandam et al., 2018).

1.3.2. Protein and peptide delivery

Drug absorption is hampered by the dissolution of stomach acid, the breakdown of digestive enzymes, and the biofilm's mechanical barrier. Only intravenous and subcutaneous injections are available for the delivery of proteins and protein and peptide medications, and these procedures sometimes necessitate long-term repeated administration, which causes patients tremendous trouble (Cao et al., 2019). The improvement of protein and peptide drug use has been made possible by the development of novel drug formulations and novel technologies; in recent years, the clinical use of novel protein drugs has been aided by nanotechnology (Cao et al., 2019).

1.3.3. Anticancer approaches

The most effective cancer treatments are targeted therapies because they are more effective than other treatments (regular chemotherapy) and cause fewer undesirable side effects, such as decreased viability, a need for lower doses, a reduction in undesirable side effects, a lack of therapeutic indicators, drug resistance, and nonspecific goals (Senapati et al., 2018). Recent research revealed that in addition to medications, imaging agents (with diagnosis capability), and genes, NPs have numerous benefits for the detection and treatment of cancers (Aghebati-Maleki et al., 2020).

1.3.4. Application against neurodegenerative disease

To stop the impending neurodegenerative disease epidemic, effective intervention is crucial. The blood-brain barrier poses limitations on CNS delivery that can be addressed by nanomedicine, which is why it is so important for preclinical research and therapeutic intervention in neurodegenerative disorders. The ability to simultaneously encapsulate many substances in regulated drug delivery systems and direct them to the deepest brain areas has been demonstrated by NPs to have significant promise and adaptability (Cano et al., 2020).

1.4. Methods of preparation of lipid NPs

Traditionally NPs were produced only by physical and chemical methods. Some of the commonly used techniques for the preparations of lipid NPs (SLNs and NLCs) are discussed below.

1.4.1. High-pressure homogenization method

SLNs, NLCs, and nanoemulsions have all been made using high-pressure homogenization (HPH). The method relies on reducing droplet and particle size at extremely high pressures (Amasya et al., 2019; Calva-Estrada et al., 2018). HPH employs two methods, hot and cold homogenization, to produce SLNs and NLCs. In hot HPH, drugs are either dissolved or uniformly dispersed in molten lipids at temperatures that are typically 5–10 °C higher than the melting point of solid lipids. Lipid content in the resulting SLNs and NLCs dispersion typically ranges between 5 and 10 % (w/v). To create a hot pre-emulsion, an aqueous phase containing surfactants is heated separately to the same temperature as the lipid melt. It is then added while being constantly stirred. At the same temperature, a piston-gap homogenizer is used to homogenise the resulting pre-emulsion. Generally, after 3–5 homogenization cycles at 500–1500 bars, the required SLNs and NLCs can be achieved. However, in highly kinetic conditions, particle coalescence may result in an increase in particle size with increasing cycle numbers and homogenization pressure (Gupta et al., 2017). When the nanoemulsions are cooled after being homogenised, lipid crystallisation takes place, forming SLNs and NLCs (Duong et al., 2020).

In order to get around some of the drawbacks of hot HPH, cold HPH was created. For cold HPH, mixtures are quickly chilled using liquid nitrogen or dry ice after medicines have been dissolved or distributed in molten lipids. Drugs in lipid matrices are dispersed uniformly thanks to this rapid cooling. The lipid-drug combinations are subsequently ground to a particle size of 50–100 m in a ball mill or a mortar. The lipid microparticles are suspended in cold aqueous solutions that contain surfactants, and they are subsequently homogenised at the cold condition (for example, 0–4 °C), typically during 5–10 cycles at 500 bars (Duan et al., 2020).

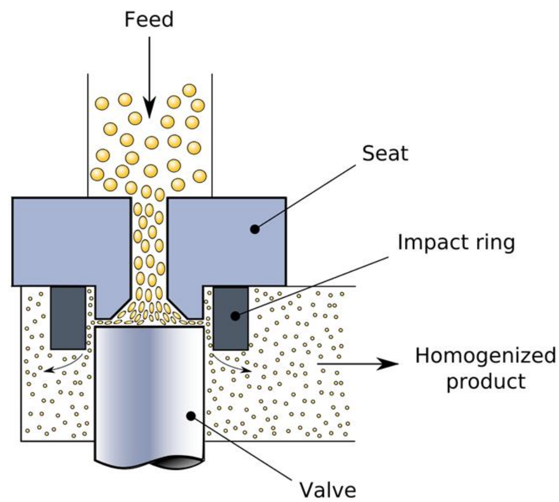

Figure 1.2. Scheme of homogenization

1.4.2. High-speed stirring and ultrasonication method

Ultrasonication and high-speed stirring (high-shear homogenization) are common dispersion methods. One of the easiest and most economical methods for creating SLNs and NLCs is high-speed stirring. This technique involves melting lipids at high temperatures (5–10 °C above the melting point of solid lipids) before dissolving or dispersing medicines uniformly inside the molten lipids. The drug-lipid melt is then combined with an aqueous phase containing surfactants (also at the same temperature), and the mixture is homogeneously dispersed using a high-shear mixer. The shear of extremely turbulent eddies leads to the formation of a hot oil/water (o/w) emulsion. These dispersions are cooled to produce SLNs and NLCs. Ultrasonication, which fractures droplets depending on the creation, development, and implosive collapse of bubbles, is typically performed after this high-speed stirring. The reason why SLNs and NLCs produced after ultrasonication without the high-shear mixing stage has a wide distribution is likely because sonication energy is not distributed equally throughout the batch. In order to produce SLNs and NLCs dispersions with narrow particle distributions, high-speed stirring and ultrasonication have frequently been utilised in conjunction (Akhoond Zardini et al., 2018; Duong et al., 2020).

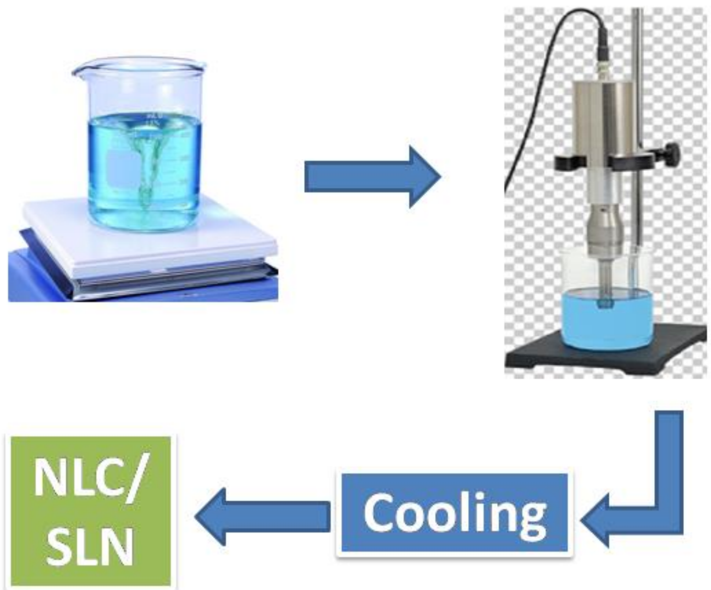

Figure 1.3. High speed stirring and ultrasonication method of preparing SLN/NLCs

1.4.3. Microemulsion method

The process includes diluting a microemulsion in a cold aqueous solution. This produces a nanoemulsion, which then causes SLNs and NLCs to develop through lipid precipitation. In a nutshell, to create a transparent and thermodynamically stable microemulsion, a drug is first dissolved in molten lipids at a temperature above the lipids' melting point. Next, a pre-heated aqueous phase comprising water and a surfactant is added while gently stirring. The microemulsion is next added to a cold (2–10 °C) water solution while being gently mechanically mixed. The cold aqueous phase typically has a volume that is 25 to 50 times larger than the hot emulsion. Lipids instantly solidify to produce SLNs or NLCs when a nanoemulsion is created as a result of dilution (Duong et al., 2020).

1.4.4. Solvent emulsification diffusion method

Common organic solvents used in this procedure include methyl acetate, ethyl acetate, isopropyl acetate, benzyl alcohol, and butyl lactate. These solvents are somewhat miscible with water. To achieve the initial thermodynamic equilibrium of both phases, the organic solvent and water are initially mutually saturated. Drugs and lipids are dissolved in the water-saturated solvent, which is then stirred into an o/w emulsion in the aqueous phase (solvent-saturated water containing stabilizer). To allow the solvent to diffuse into the continuous phase, the emulsion is diluted with water (1:5 to 1:10). Lyophilization or vacuum distillation is used to get rid of the solvent after SLNs and NLCs spontaneously form as a result of lipid precipitation (Duong et al., 2020).

1.4.5. Solvent emulsification evaporation method

The solvent emulsification-evaporation approach is utilized to create SLNs and NLCs, as opposed to the emulsification-diffusion method, which uses water-immiscible organic solvents (such as chloroform, cyclohexane, dichloromethane, and toluene). In a nutshell, to create nanodispersions, medicine and lipids are first dissolved in a solvent or a solvent mixture, and then they are emulsified in an aqueous phase. The organic solvent is then evaporated either in a rotary evaporator or by mechanical stirring. After solvent evaporation, lipid precipitation causes the formation of SLNs and NLCs (Patel et al., 2019). This technique is advantageous for encapsulating extremely thermo-labile pharmaceuticals since it minimizes drug exposure to high temperatures. SLNs and NLCs made with this method as well as the solvent emulsification-diffusion method also had narrow size distributions and particles of about 100 nm. The solvent emulsification-evaporation method has some drawbacks, including the need for hazardous organic solvents and the diluted suspension generated, which needs additional evaporation or ultra-filtration (Duong et al., 2020).

1.4.6. Double emulsion method

The double emulsion technique enables the SLN and NLCs synthesis of hydrophilic pharmaceuticals and biomolecules (e.g., peptides and proteins). It has been extensively employed, in particular, to include insulin in the matrices of SLNs and NLCs for oral delivery. This technique involves dissolving a medication and a stabilizer in an aqueous solution, followed by emulsification in a water-immiscible organic phase that contains lipids or in molten, solvent-free lipids (Mazur et al., 2019). Water/oil/water (w/o/w) emulsion is created by dispersing these primary emulsions in an aqueous phase that also contains a hydrophilic emulsifier. Lipid precipitation results in the formation of SLNs and NLCs dispersions following solvent evaporation. Notably, the stabilizer for this approach effectively precludes drug partitioning to the external water phase after solvent evaporation (Duong et al., 2020).

1.4.7. Phase inversion temperature (PIT) method

It has been possible to create nanoemulsions, SLNs, and NLCs using the PIT approach. The method is based on the w/o to o/w emulsions' temperature-induced inversions and vice versa. Non-ionic polyoxyethylated surfactants with temperature-dependent characteristics are required for the process. These surfactants have a high hydrophilic-lipophilic balance (HLB) value at low temperatures due to their highly hydrated hydrophilic groups. Dehydration of the ethoxy group happens with rising temperature, increasing surfactant lipophilicity and lowering the surfactants' HLB values. When the affinities of the surfactants for the aqueous and lipid phases are similar, that temperature is known as PIT. Surfactants enhance the production of w/o emulsions at temperatures over PIT, whereas at temperatures below PIT, they start to create o/w emulsions. Oil, water, and surfactant are heated to a temperature > PIT while being stirred to make emulsion-free SLNs and NLCs. They are then quickly cooled while being stirred continuously, which encourages the breakdown of w/o microemulsions and encourages the production of o/w nanoemulsions. When lipids are precipitated at low temperatures, SLNs and NLCs are created (Duong et al., 2020).

1.4.8. Membrane contactor method

This approach creates SLNs and NLCs using a certain membrane contactor. In a nutshell, a lipid phase is forced through a membrane's pores while the temperature is kept above the lipid's melting point. The creation of tiny droplets is the result of this process. Within a module, a surfactant-containing aqueous phase circulates over the other side of the membrane at the same time. It washes away the droplets that have accumulated at pore outputs as it flows tangentially to the membrane surface. By allowing the hot emulsion to cool to room temperature, SLNs and NLCs are created. In-depth research is being done on the effects of formulation and process parameters, such as membrane pore size, lipid phase pressure, aqueous phase flow velocity, and aqueous and lipid phase temperatures, on the size of SLNs and NLCs. By altering the lipid phase transit through membranes, particle size can be changed (Duong et al., 2020).

1.4.9. Supercritical fluid-based method

Supercritical fluids, such as supercritical CO_2, were used in several SLNs and NLCs production processes. The o/w emulsion is created first for the supercritical fluid extraction of emulsions (SFEE) method, which is followed by the supercritical fluid extraction of the organic solvent. Typically, supercritical CO_2 is injected in a counter-current way from the bottom of an extraction column while the emulsion is added to it from the top. When compared to alternative techniques that rely on evaporation, diffusion, and dilution, SFEE has a significantly better solvent extraction efficiency. Lipid precipitates as a result of the rapid and complete solvent removal. Additionally, the SLNs and NLCs that were created had a consistent particle size distribution (Andrade et al., 2019).

1.4.10. Coacervation method

This approach is based on the alkaline fatty acid salts precipitating as a result of acidification. The lipids are distributed in an aqueous solution of a polymeric stabilizer, such as PVA or HMPC, and come in the form of alkaline salts (for instance, sodium stearate). In subsequent processes, drugs can be put into blank SLNs or dissolved in the lipid phase (Battaglia et al., 2017; Clemente et al., 2018). Drugs are solubilized in ethanol and then dissolved in the lipid to load them into the lipid phase. When the combination is heated above the Krafft point, the lipid alkaline salts dissolve into a transparent micellar solution. The lipids then precipitate when an acidifying solution (coacervating solution) is added dropwise to this solution. After reaching a temperature of 15 °C, the acquired suspension is cooled in a water bath while being stirred at 300 rpm to finish the precipitation of SLNs or NLCs (Duong et al., 2020).

1.4.11. Solvent injection method

This procedure involves dissolving lipids and medications in a water-miscible solvent or a water-miscible solvent mixture, such as methanol, ethanol, isopropanol, or acetone. Typically, an emulsifier or emulsifier mixture is added to water or a buffer solution to prepare the aqueous phase. The aqueous phase is then rapidly infused with the organic phase while being continuously mechanically stirred. This technique and the solvent emulsification-diffusion technique have similar fundamental ideas (Duong et al., 2020).

1.5. Characterization of NPs

Characterization of NPs is carried out using the following methods.

1.5.1. Drug loading and encapsulation efficiency

Utilizing an ultraviolet (UV) spectrophotometer to measure the absorbance at a certain range allows for the analysis of the amount of drug loaded within NPs (Rapalli et al., 2020). The percentage of drug loading (DL) is calculated by using the following formula:

$$\text{DL (\%)} = (\text{Weight of the drug in NPs/Weight of NPs}) \times 100$$

$$\text{EE (\%)} = (\text{Weight of drug in NPs/ Weight of drug used to formulate NPs}) \times 100$$

1.5.2. Particle size and size distribution

Particle size and surface morphology are very important parameters of nanostructured lipid carriers. The significant therapeutic parameters such as dissolution, permeation, cellular uptake, bioavailability, clearance etc. depend on surface morphology and particle size. These properties are estimated by dynamic light scattering (DLS) and microscopic techniques.

NPs' particle size is determined using the DLS technique. DLS calculates the hydrodynamic size of particles, taking into account their surface coating and solvent layer. DLS is a technique that relies on how light interacts with particles. DLS mainly depends on Rayleigh scattering from the suspended NPs to determine the light scattered from a laser that passes through a colloid.

This technique can be used to measure small particle size distributions, particularly in the 2-500 nm range (Caputo et al., 2019).

1.5.3. Surface charge

Zetasizer is used to determine the surface charge of the produced NPs. A DLS instrument can be used to test the zeta potential of NPs in various aqueous dispersion media, including phosphate buffer solution (PBS), cell culture medium, and water, and to investigate the surface charge properties. The stable dispersion of NPs in aqueous media is determined by the value of zeta potential (Pochapski et al., 2021).

1.5.4. Surface morphology

Scanning electron microscope (SEM) is a tool that has been employed across a wide range of fields. On a nanoscale to micrometre (nm–µm) scale, it can be regarded as an efficient approach for the analysis of organic and inorganic materials. With a high magnification that can reach 300,000x and even 1,000,000x (in some recent models), SEM creates extremely exact images of a variety of materials (Mohammed and Abdullah, 2018). The nanomaterials are suitably coated and observed with SEM to determine the surface characteristics and size of the nanomaterials.

1.5.5. Particle morphology

Transmission electron microscopy (TEM), which has made great strides in spatial resolution, has been able to probe enhanced information about materials at the atomic scale (Lin et al., 2021). The nanomaterials are loaded on a TEM grid using the drop cast method and analyzed with an electron beam to identify the shape and particle morphology.

1.5.6. Surface topography

Using an atomic force microscope, three-dimensional images are obtained by measuring the interaction forces between the tip and the sample.

1.5.7. Drug release characteristics

The *in vitro* drug release is quantified employing UV-visible spectroscopy or high-performance liquid chromatography (HPLC) (Kim et al., 2021). Drug release assays are also similar to drug loading assays, which are assessed for a period of time to analyze the mechanism of drug release. Drug release mechanisms are important parameters of NPs as it mimics the conditions under which the nanoformulations are subjected and the observations provide information about the bioavailability of drug across membrane barriers. Usually, membranes which are comparable to cell membranes are used in drug release assays (eg. dialysis membranes). NPs are enveloped in the membrane pouch and placed within a blood-like fluid which is kept flowing using mechanical stirrers. Data obtained can be fitted to various pharmacokinetic models to determine the best fit.

Chapter 2

Literature Review

Contents

2. Literature review

The in depth literature survey is required before executing any research work. Review of literature includes gathering all the appropriate information related to the research materials and research methodologies. Over past few decades, World Wide Web can give up-to-date information of all the appropriate literature within a brief span of time. This chapter depicts all the relevant information of test materials to justify their crucial roles in the preparation of NPs.

2.1. Literature review of Mgn

Mgn (1,3,6,7-tetrahydroxyxanthone-C2D-glucoside) is a bioactive substance that is primarily isolated from *Mangifera indica*. It has potent antioxidant activity as well as a variety of pharmacological effects, including anti-diabetic, anti-tumor, cardioprotective, anti-hyperuricemic, neuroprotective, anti-inflammatory, antipyretic activities (Du et al., 2018). As a result, it has a number of health-promoting qualities thus offering a viable subject for further study and development. However, the development of Mgn as a clinical therapy is constrained by its low solubility, mucosal permeability, and bioavailability, and chemical and physical modification is needed to broaden its application (Du et al., 2018).

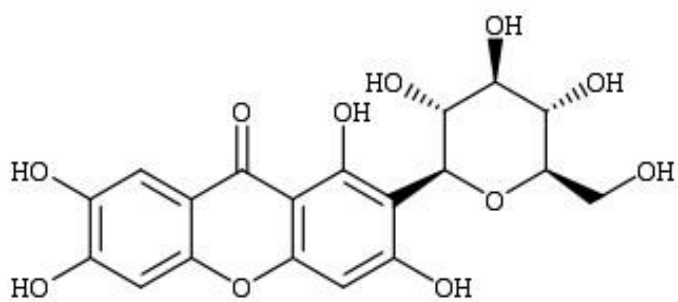

Figure 2.1. Chemical structure of Mgn

2.1.1. Physicochemical Characteristics

Molecular formula: $C_{19}H_{18}O_{11}$

Molecular weight (MW): 422.3

IUPAC name: 1,3,6,7-tetrahydroxy-2-[(2*S*,3*R*,4*R*,5*S*,6*R*)-3,4,5-trihydroxy-6-(hydroxymethyl) oxan-2-yl]xanthen-9-one

Solubility: Mgn is slightly soluble in ethanol, sparingly soluble in methanol and water and practically insoluble in diethyl ether, acetone, and n-hexane (Acosta et al., 2016). Mgn is freely soluble in DMSO and dimethyl formamide (Du et al., 2018).

2.1.2. Pharmacological properties

Antioxidant, antibacterial, antidiabetic, antiallergic, neuroprotective, cardioprotective, anticancer, hypocholesterolemic, and immunomodulatory activities are exhibited by Mgn. Mgn is thought to have a wide range of pharmacological activities However, since the majority of these effects have only been shown in *in vitro* investigations, more clinical study into the pharmacology and pharmacokinetics of Mgn is necessary. Mgn administration to humans or animals will unavoidably cause changes in the body at the molecular, cellular, tissue, and/or organ levels in addition to its therapeutic benefits. Therefore, the primary methods used to ascertain the pharmacodynamics of Mgn should be genomic, proteomic, and metabolomic studies (Du et al., 2018).

2.1.2.1. Antidiabetic effect

Diabetes-prone mice treated with Mgn had significantly lower blood sugar, glycosylated haemoglobin, aspartate aminotransferase (AST), alanine aminotransferase (ALT), and alkaline phosphatase (ALP) levels than diabetic control mice (Sellamuthu et al., 2014). Additionally, there was a noticeable improvement in the numbers of red and white blood cells (Sellamuthu et al., 2014; Sellamuthu et al., 2009). Thus, in chemically induced diabetic mice, Mgn was shown to have anti-diabetic activity without harm. Mgn was also shown to simultaneously reduce triglyceride (TG), total cholesterol (TC), and low-density lipoprotein cholesterol (LDL-C) levels in the serum, as well as the atherogenic index, liver TG and liver TC content, in a high-fat, high-fructose diet and STZ-induced diabetic insulin-resistant rat model of diabetes. Additionally, liver glycogen content increased (Saleh et al., 2014). These findings supported the possibility that Mgn may successfully increase insulin sensitivity in the treatment of type 2 diabetes in conjunction with metabolic abnormalities.

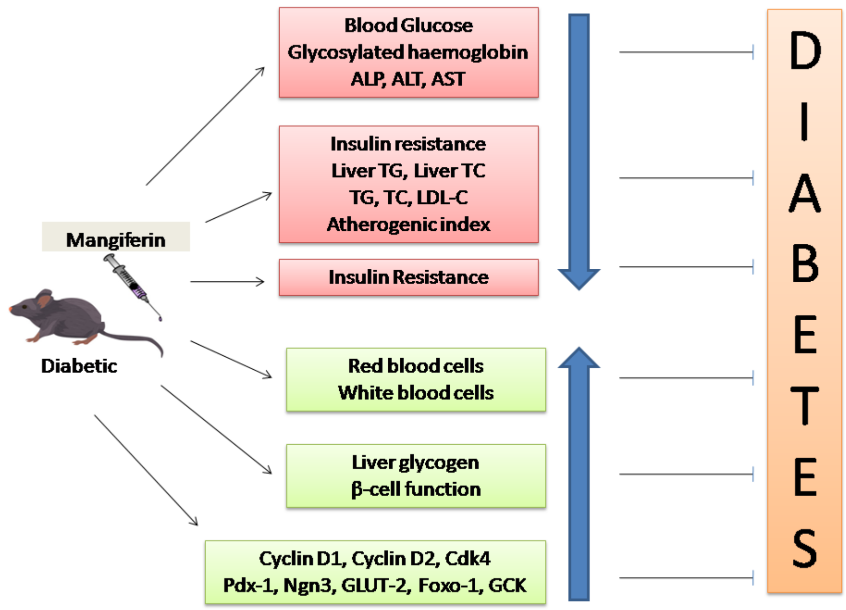

Figure 2.2. Mechanisms of action of anti-diabetic activities of Mgn

2.1.2.2. Anticancer effect

It is commonly acknowledged that the cyclin-dependent kinase 1 (CDK1)/cyclin B1 complex tightly regulates cell proliferation before cell division. Notably, Mgn has been shown to cause cell cycle arrest in the G2/M phase via controlling the CDK1-cyclin B1 signaling pathway (Yao et al., 2010; Hu and Moscinski, 2011; Peng et al., 2015). In colorectal cancer HT29 cells and cervical cancer HeLa cells, treatment with Mgn delays the S phase of the cell cycle, which is when DNA synthesis is completed (du Plessis-Stoman et al., 2011). However, a collective patent study on Mgn revealed that the anticancer actions of Mgn involve a number of signalling pathways, including nuclear NF-κB signaling and the production of the COX-2 protein (Telang et al., 2013). Additionally, the apoptosis-inducing effects of Mgn in oncotherapy may involve caspase activation. Mgn has been shown by Pan et al. (2014) to potently suppress tumour cell proliferation and cause apoptosis in nasopharyngeal cancer cells by modulating the expression of the apoptosis regulators Bcl-2 and Bcl-2 associated X. Additionally, a study of the antitumor effectiveness and underlying mechanisms of Mgn in human cervical carcinoma HeLa cells showed that the protein expression of BH3 interacting domain death agonist, Bcl-2, and pro-caspase-3 and -8 is downregulated in response to Mgn treatment. This causes caspase-3, -7, -8, and -9 to be activated, which ultimately induces apoptosis (Kim et al., 2012).

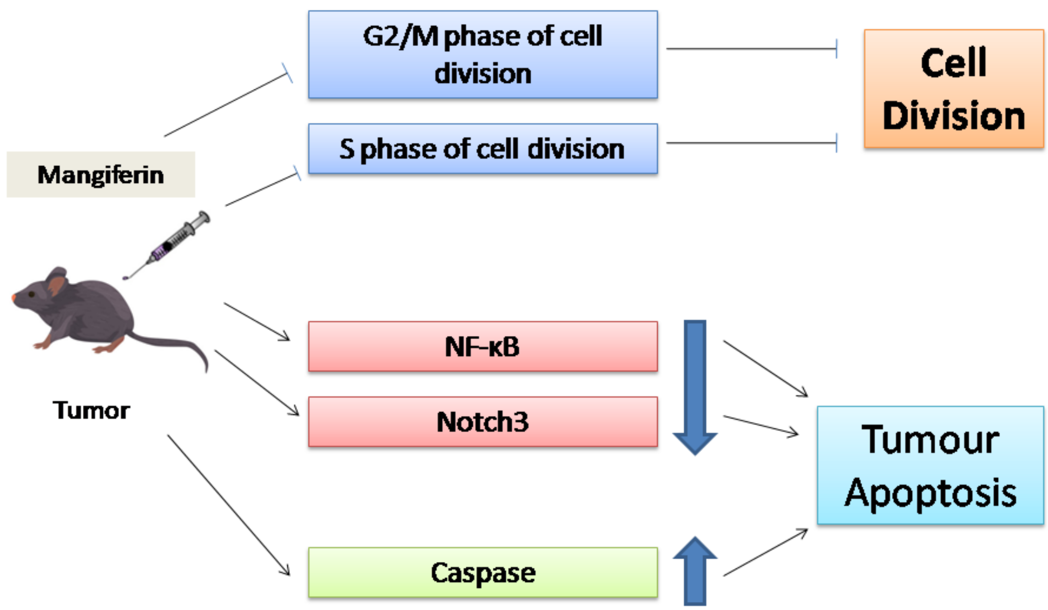

Figure 2.3. Mechanisms of action of Mgn as anti-cancer agent

2.1.2.3. Neuroprotective effect

Due to its C-glycosylxanthone structure, extensive study on the effects of Mgn has revealed its antioxidant and anti-inflammatory characteristics. Mgn's polyhydroxy component and C-glucosyl linkage both contribute to its capacity to scavenge free radicals (Saha et al., 2016). By combining research on oxidative stress, inflammation, and other pathogenic processes like excitotoxicity, calcium overload, mitochondrial cytochrome c release, caspase activation, and apoptosis in trauma and ischemia of the central nervous system, the role of free radicals in the pathology of traumatic brain injury and cerebral ischemia has been clarified in recent decades (Lewén et al., 2000). Additionally, Mgn has the ability to regulate a number of transcription factors, including NF-κB and NF-E2-related factor 2 (Nrf-2), as well as the production of proinflammatory signalling molecules, such as TNF-α and COX-2 (Saha et al., 2016). In mice, oral Mgn pre-treatment at 50 mg/kg and therapy at 50 mg/kg after LPS injection showed that Mgn reduces LPS-induced IL-6 expression and increases the expression of heme oxygenase-1 (HO-1) in the hippocampi. Similar to this, in behavioural trials, mice were pretreated orally with Mgn (20 and 40 mg/kg, 14 days) before receiving LPS (0.83 mg/kg), which subsequently reduced depression and anxiety-like behaviours (Jangra et al., 2014). Mgn also lessens oxidative stress and IL-1 expression that are caused by LPS when used to treat depression and anxiety disorders (Jangra et al., 2014). Mgn ameliorates neurological impairments and brain edoema, lessens SAH-induced oxidative stress, and reduces cortical cell death in a dose-dependent manner. It also reduces the mortality of rats with SAH. The nuclear factor erythroid 2-related factor 2 (Nrf2)/HO-1 cascade in the mitochondrial apoptotic pathway, as well as NLRP3 inflammasome activation and NF-KB inhibition, are the mechanisms by which Mgn exerts its neuroprotective effects against EBI (Wang et al., 2017).

2.1.2.4. Cardiovascular effect

There is growing evidence that Mgn possesses cardioprotective properties in rats with myocardial infarction (MI) produced by isoproterenol (ISPH). Mgn (100 mg/kg) pretreatment for 28 days has been shown by Prabhu et al. (2006) to control the tissues' defensive mechanism against cardiac injury. Particularly, the activities of non-enzymic antioxidants like cerruloplasmin, vitamin C, vitamin E, and glutathione as well as enzymatic antioxidants found in heart tissue such as superoxide dismutase, catalase, glutathione peroxidase, glutathione transferase, and glutathione reductase were all significantly upregulated (Prabhu et al., 2006). It was determined that Mgn's antioxidant capacity, which lowers myocardial oxygen consumption and alleviates angina pectoris, is how it exerts its positive benefits (Prabhu et al., 2006). Mgn also shields the myocardium against MI brought on by ISPH by lowering the production of lipid peroxide and maintaining the activity of cardiac marker enzymes such as LDH, creatine phosphokinase (CPK), AST, and ALT (Prabhu et al., 2006a). According to those findings, Mgn efficiently reduces the release of free radicals in the ischemic myocardium and postpones membrane lipid oxidation. Mgn also maintains structural integrity by lowering the effects of oxidative damage and enhancing mitochondrial energy metabolism, according to investigations in cardiac cells subjected to ISPH-induced MI (Prabhu et al., 2006b). In MI, Mgn significantly boosts the tricarboxylic acid cycle and antioxidant defence enzyme activity (Prabhu et al., 2006b). Mgn has also been shown to increase lysosomal instability and stop free radical-mediated lipid peroxidation, which reduces MI harm (Prabhu et al., 2009). Mgn has been shown to reduce excessive cellular permeability and endothelial damage brought on by paraquat toxicity in HUVECs by modification of the p120-catenin protein. In addition, Mgn administration improves cell survival in H2O2-treated HUVECs by scavenging free radicals. Its antioxidant capacity was further confirmed by a ferric reduction ability of the plasma test (Luo et al., 2012).

2.1.2.5. Respiratory effects

Mgn protects against allergic disorders including bronchial asthma and other allergic conditions. Mgn reduces tracheal contractions brought on by several stimuli, including as allergens, histamine, 5-hydroxytryptamine, and carbachol, in a dose-dependent way.

According to a research, Nitric oxide synthase 3 and cyclic GMP levels are elevated intracellularly, which has an antispasmodic impact on allergic and non-allergic tracheal contraction in guinea pig tracheal rings when Mgn is administered (Vieira et al., 2013). Additionally, mice were given oral treatments with Mgn (50 mg/kg) or *M. indica* extract (50, 100, or 250 mg/kg) from day 0 to day 24 in an allergic murine experimental model. According to the findings, Mgn significantly reduces inflammation surrounding blood vessels and bronchi, as well as immunoglobulin (Ig)E levels and lymphocyte proliferation. Mgn was also shown to decrease the generation of IL-4 and IL-5 cytokines in lymphocyte culture supernatant and bronchoalveolar lavage fluid (Rivera et al., 2011). These studies may play a significant role in the pre-clinical research required for the use of Mgn in the treatment of respiratory illnesses.

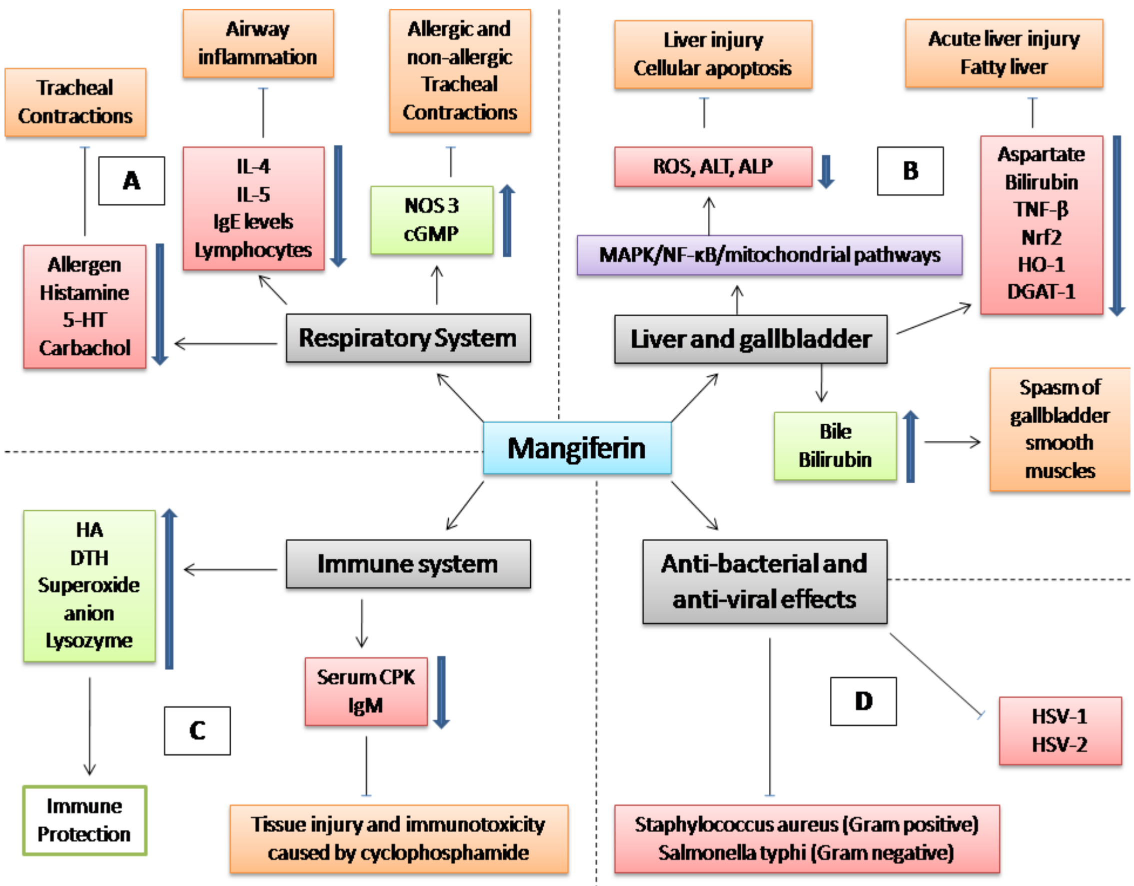

Figure 2.4. Mechanisms of action of Mgn against respiratory disorders (A), against liver and gallbladder disorders (B), immunomodulatory effects (C), and anti-bacterial and anti-viral actions (D)

2.1.2.6. Mgn in liver and gallbladder disorders

The molecular mechanisms behind Mgn's preventive activity against lead-induced liver damage and cellular apoptosis were examined by Pal and colleagues (2013). Mgn (100 mg/kg, taken orally for 6 days) was found to suppress the generation of ROS and lower levels of blood marker enzymes including ALT and ALP. Overall, it was shown that Mgn acts through mitochondria-dependent pathways to exhibit antioxidative and antiapoptotic characteristics (Pal et al., 2013). Mgn (30 mg/kg) administered intraperitoneally prior to silymarin, a common hepatoprotective medication, has a more comprehensive protective effect by lowering serum levels of the inflammatory mediators TNF-α and aspartate and alanine aminotransferases as well as alkaline phosphatase and bilirubin. These findings imply that Mgn has strong liver-protective effects on mouse liver damage brought on by CCl_4 (Rasool et al., 2012). Mgn also dose-dependently upregulates the expression of Nrf2 and HO-1 in acute liver damage caused by LPS and D-galactosamine (D-GalN). Mgn also significantly reduces the inflammatory factors that LPS/D-GalN induces, such as IL-1, TNF, NLRP3, apoptosis-associated speck-like protein with a CARD, and caspase-1 (Pan et al., 2016).

2.1.2.7. Immunomodulating property

Mangifera indica (extract containing 2.6 percent Mgn) has been studied for its immunoprotective properties by raising the frequency of mice's humoral antibody (HA) titer and delayed-type hypersensitivity (DTH) reactions (Makare et al., 2001). It was proposed that the components of Mangifera indica extracts may be of potential value for modulating the humoral response in various immunopathological disorders after comparing the immunoprotective effects of Mgn (the major polyphenol of Vimang) and VIMANG (an aqueous extract of Mangifera indica) on mouse antibody responses induced by inoculation with spores of microsporidian parasites (García et al., 2003). However, in addition to the Mgn polyphenol, VIMANG also contains other extracts, thus it's possible that the researchers overlooked the humoral response-inhibiting properties of other chemicals extracted from VIMANG (García et al., 2003). Mgn also significantly inhibits the immunotoxicity and tissue damage brought on by cyclophosphamide treatment by lowering serum CPK activity and antigen-specific IgM levels (Muruganandan et al., 2005). Therefore, it was clear that Mgn inhibits reactive intermediate-induced oxidative stress in lymphocytes, neutrophils, and macrophages, which plays an immunoprotective role (Muruganandan et al., 2005). According to these findings, Mgn may be able to lessen the immunotoxicity of cyclophosphamide when used in oncotherapy.

2.1.2.8. Antimicrobial and antiviral properties

Mgn has significant antibacterial and antiviral effects in addition to its antioxidant, antidiabetic, and antitumor properties. Gram-negative *Salmonella typhi* and Gram-positive *Staphylococcus aureus* are the two bacterial species against which Mgn has been shown to have antibacterial activity (Biswas et al., 2015). With average plaque reduction rates of 56.8 and 69.5 percent, respectively, Mgn and isoMgn were found to have antiviral effects on herpes simplex virus-1 (HSV-1) in tissue culture (Zheng and Lu, 1990). By blocking mast cell degranulation, lowering blood levels of specific anti-Trichinella IgE, and reducing the number of parasite larvae, oral Mgn (50 mg/kg) inhibits the growth of the worm *Trichinella spiralis* throughout the parasitic life cycle (García et al., 2003). These investigations support isolated Mgn's antibacterial properties, which may be further processed to create an antibacterial agent. A study showed that Mgn exerted synergistic antibacterial effect on S. aureus when used in combination with four standard antibiotics: nalidixic acid, ampicillin, tetracycline, and sulfamethoxazole/trimethoprim (Mazlan et al., 2019). Results of another study showed interesting antibacterial properties associated with the oxide precursor and the charge, shape, and size of the NPs (Razura-Carmona et al., 2022). Mgn incorporated in Pluronic lecithin organogel showed antiviral effects against HSV-1 KOS strain (Sicurella et al., 2021).

2.2. Literature review of lipids (beeswax and olive oil)

The western honey bee (*Apis mellifera L.*) produces its wax utilizing four pairs of specialized wax glands that are situated on the inner side of the fourth through seventh abdominal sternites. This wax is a complex lipid-based organic molecule known as natural wax. Honey bees exude beeswax in the form of wax scales, which they transfer with their forelegs to their mandibles where they are chewed (adding salivary secretions), before adding the scales to the comb that is being built. This mandibulation method converts the texturally anisotropic scale wax into isotropic comb wax as its primary result (Svečnjak et al., 2019). More than 300 different chemicals make up beeswax chemically, with fatty acid esters (67%), hydrocarbons (14%), and free fatty acids (13%) dominating the mixture (Svečnjak et al., 2019). Beeswax has long been used for a variety of practical purposes, including embalming, papyrus preservation, painting protection, candle-making, making figurines and ancient seals, and as a component in medicines and adhesives. The bulk of beeswax produced today is utilized to make comb foundations, bringing the beekeeping business back into existence. The creation of comb foundations is most likely the primary usage of beeswax, despite the fact that accurate statistics on beeswax production and statistics on global trade for beeswax-based goods are difficult to come by. Additionally, beeswax is widely utilized in the cosmetics, food, and pharmacy industries (Svečnjak et al., 2019).

The olive tree, or *Olea europaea L.*, is a tiny tree species that is mainly found in Mediterranean nations. Due to its organoleptic properties and the related positive health consequences, olive oil, its principal-derived product, has seen an increase in popularity (Foscolou et al., 2018). This relationship is mostly caused by the unique biological characteristics and content of the substance. Triglycerides, along with a number of other minor amounts of other chemicals, make up the majority of the content of olive oil. Olive oil exhibits a high amount of fatty acids and, in particular, a significant proportion of monounsaturated fatty acids (MUFA) within the glyceride fraction. Due to its high level of oleic acid (C18:1), which may vary between 70 and 85 %, and other fatty acids like linoleic or palmitoleic acid, unsaturated acids account for up to 85 % of its composition. Saturated fatty acids make up about 14% of the oil makeup in this case, primarily attributable to palmitic and stearic acids (Jimenez-Lopez et al., 2020). Minor compounds make up less than 2% of the content of olive oil, and phenolic compounds are its best representatives. However, this minor group also contains some lipophilic compounds, such as α-tocopherol (vitamin E). The simple phenol hydroxytyrosol and the secoiridoid oleuropein, which are among the hydrophilic phenolic chemicals, must be highlighted (Foscolou et al., 2018). Besides having beneficial qualities, olive oil can also be used as a liquid lipid for the formation of NPs (Saporito et al., 2017).

2.3. Literature review of PVA

Commercially, it is made from polyvinyl acetate, typically using a continuous process. In the presence of either anhydrous sodium methylate or aqueous sodium hydroxide, the acetate groups are hydrolyzed via ester interchange with methanol. The degree of polymerization and the degree of hydrolysis determine the physical properties and the specific functional applications (Nagarkar and Patel, 2019). It is mildly soluble in ethanol and soluble in water, but it is insoluble in other organic solvents. A 5 percent solution of PVA typically has a pH between 5.0 and 6.5 (Nagarkar and Patel, 2019). The formula for PVA is $(C_2H_4O)_n$. For commercially accessible materials, the degree of polymerization ranges from 500 to 5,000, or MW of 20,000 to 200,000 (Nagarkar and Patel, 2019). Other PVA characteristics, including as bio-inertness and compatibility, have consequences for advanced medical applications like hemodialysis, drug delivery systems, and implantable medical devices (Chen et al., 1994; Lee et al., 2012). It serves as a moisture barrier coating for foods that need to be protected from moisture absorption, such as inclusion-containing foods and dry foods (Nagarkar and Patel, 2019). PVA-based polymers are employed as drug carriers in the pharmaceutical and medicinal disciplines and in the science of tissue engineering (Kayal and Ramanujan, 2010; Sirousazar et al., 2011; Salunkhe et al., 2013).

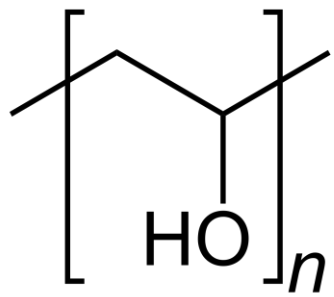

Figure 2.5. Repeating unit of PVA

2.4. Literature review on the success of NLCs

In a study, a stable NLCs system that acts as a curcumin carrier is developed. The curcumin-loaded NLCs crystallized as a particle with the following properties: 146.8 nm in size, 0.18 polydispersity index, 90.86 % entrapment efficiency, and 21.4 mV zeta potential. Additionally, it was found that curcumin-NLCs were more harmful to the astrocytoma-glioblastoma cell line (U373MG) in the cancer cell lines than curcumin was. When NLCs were administered intranasally as opposed to a free drug suspension, the results of biodistribution tests revealed a greater drug concentration in the brain. The study's findings further imply that curcumin-NLCs are a promising medication delivery technology for the treatment of brain cancer (Madane et al., 2016).

Acitretin-NLCs were created utilizing a 3^2 complete factorial design and the solvent diffusion approach. Acitretin-NLCs’ average diameter and surface morphology were assessed. ActNLCs were lyophilized, and powder XRD and DSC were used to determine the crystallinity of the NLCs. The NLCs were added to the Carbopol 934 P gel basis at a concentration of 1 % by weight, and research on the in vitro skin deposition in human cadaver skin as well as double-blind clinical trials in psoriatic patients were carried out. The optimised ActNLCs had a zeta potential of 26.4 (0.86) mV, an average particle size of 223

(8.92) nm, and an efficiency of 63.0 (1.54) percent. The development of NLCs was confirmed by XRD and DSC measurements. Acitretin-NLCs gel significantly increased the amount of retinol that was deposited in the skin of human cadavers (81.38 vs. 1.23 percent vs. 47.28 vs. 1.02 percent). With Acitretin-NLCs loaded gel, clinical investigations showed a significant improvement in therapeutic response and a decrease in local adverse effects, demonstrating its efficacy in the topical treatment of psoriasis (Agrawal et al., 2010).

In another study, a high pressure homogenization process was used to prepare vinpocetin-loaded NLCs. Under the investigation of the TEM and SEM, the vinpocetin-NLCs displayed spherical morphology with a smooth surface. Encapsulation efficiency on average was 94.9 minus 0.4 percent. By using DSC and powder XRD, the drug's crystallization in NLCs was examined. In the NLCs matrix, the drug was in an amorphous condition. The in vitro release analysis conducted on vinpocetin-NLCs revealed a continuous release profile of vinpocetin and no blatant burst release was noticed. Wistar rats were used in the research of vinpocetin's oral bioavailability. Compared to vinpocetin suspension, vincopocetin-NLCs had a 322 percent higher relative bioavailability. In conclusion, the NLCs formulation significantly increased the oral bioavailability of vinpocetin and showed a promising future for the oral delivery of medicines that are not well soluble in water (Zhuang et al., 2010).

Bacterial endophthalmitis (BE) is an inflammatory response to intraocular fluids or tissues that can be sight-threatening. As the initial line of treatment, BE prescribes ciprofloxacin (CIP) eye drops. However, frequent administration is necessary due to precorneal loss and poor ocular bioavailability. Preparing CIP comprising NLCs (CIP-NLCs) loaded with in situ gel system (CIP-NLCs-IG) for topical ocular administration with increased and prolonged antibacterial activity in BE treatment was the main goal of the current study. The heat homogenization process was used to create CIP-NLCs, which were then adjusted based on their physicochemical properties and physical stability. With the addition of gellan gum as a gelling agent, the optimized CIP-NLCs formulation was changed into CIP-NLCs-IG. Additionally, using commercial CIP ophthalmic solution (CIP-C) as the control, optimized CIP-NLCs and CIP-NLCs-IG were assessed for in vitro release and ex vivo transcorneal permeation experiments. The particle size, polydispersity index, zeta potential, assay, and entrapment efficiency of the optimized CIP-NLCs formulation were 193.1 ± 5.1 nm, 0.43 ± 0.01, 32.5 ± 1.5 mV, 99.5 ± 5.5, and 96.3 ± 2.5 %, respectively. Gellan gum at 0.2 % w/v in CIP-NLCs-IG demonstrated the best viscoelastic properties. The in vitro release tests showed that CIP from CIP-NLCs and CIP-NLCs-IG formulations released continuously for 24 hours.

When compared to CIP-C, the transcorneal flow and permeability of the CIP-NLCs and CIP-NLCs-IG formulations, respectively, rose by 4 and 3.5 and 2.2 and 1.9 times, respectively. The outcomes show that CIP-NLCs-IG may be used as a different delivery method to extend the period that a topical medication stays on the ocular surface after application. As a result, the current CIP ophthalmic formulations might have enhanced ocular bioavailability and sustained antibacterial activity, which might enhance therapeutic results in the management of BE (Youssef et al., 2020).

The solubility and oral biological availability of 6-gingerol (6G), an active and abundant component of ginger with few applications due to its poor water solubility and oral biological availability, were improved in a study using an optimised NLCs. The NLCs were made by high pressure homogenization and included a liquid lipid (decanoyl/octanoyl-glycerides), a solid lipid (glyceryl monostearate), and a mixture of surfactants (Tween 80 and Poloxamer 188). TEM, DSC, and powder XRD techniques were used to assess physical properties such as appearance, mean particle size, zeta potential, encapsulation effectiveness, and in vitro drug release in order to determine the best 6G-NLCs formulation. Rats were used to examine pharmacokinetics. The 6G-NLCs made with the best formulation had a mean particle size and zeta potential of 63.59 ± 5.54 nm and 12.18 ± 1.06 mV, respectively, and were uniformly spherical in shape. The percentages of drug loading and encapsulation efficiency were 1.17 and 0.35 respectively. 6G's sustained *in vitro* release profile from NLCs was fitted with the Weibull equation. Drug concentrations in serum, MRT, and $AUC_{0\text{-}t}$ were considerably higher following oral administration of the 6G-NLCs than they had been following oral administration of the free 6G solution. These findings suggested that the created NLCs formulation might function as an efficient and promising drug carrier to boost the water solubility of 6G while maintaining drug release, extending the drug's in vivo action time, and improving oral bioavailability (Wei et al., 2018).

2.5. Literature review on the stirring-ultrasonication method

Ultrasonication and high-speed stirring (high-shear homogenization) are common dispersion methods. One of the simplest and most affordable methods for creating SLNs and NLCs is high-speed stirring (Das et al., 2011). This technique involves melting lipids at high temperatures (5–10 °C above the melting point of solid lipids) before dissolving or dispersing medicines uniformly inside the molten lipids. The drug-lipid melt is then combined with an aqueous phase containing surfactants (also at the same temperature), and the mixture is homogeneously dispersed using a high-shear mixer. The shear of extremely turbulent eddies leads to the formation of a hot oil/water (o/w) emulsion. These dispersions are cooled to produce SLNs and NLCs (Severino, et al., 2012; Souto et al., 2019). Ultrasonication, which fractures droplets depending on the creation, development, and implosive collapse of bubbles, is typically performed after this high-speed churning. The reason why SLNs and NLCs produced after ultrasonication without the high-shear mixing stage have a wide distribution is likely because sonication energy is not distributed equally throughout the batch. In order to produce SLNs and NLCs dispersions with narrow particle distributions, high-speed stirring and ultrasonication have frequently been utilized in conjunction (Fazly Bazzaz et al., 2018; Akhoond Zardini et al., 2018; Tamjidi et al., 2014). The preparation of lycopene-loaded SLNs and NLCs involved high-speed stirring (20,000 rpm for 1 min) and subsequent ultrasonication (about 4 min), which resulted in particles of 200 nm or less and polydispersity indices (PDIs) of 0.22 to 0.32. Monostearin and medium-chain triglycerides were the lipids employed (Akhoond Zardini et al., 2018). Without using organic solvents, both ultrasonication and high-speed stirring are simple to employ and have a wide range of applications (Jannin et al., 2018).

Chapter 3

Aims and Objectives

Contents

3.1. Aims

The aim of the study is to develop, optimize, and characterize the Mgn-NLCs for improving the therapeutic potential of Mgn.

3.2. Objectives

- To develop and optimize Mgn-loaded NLCs to overcome biopharmaceutical incompetence of Mgn.
- To achieve better therapeutic efficacy of Mgn against breast cancer cells.
- To reduce loss and dose amount with nanoformulation compared to free drug.
- To obtain the controlled release of Mgn from the formulation.

3.3. Plan of work

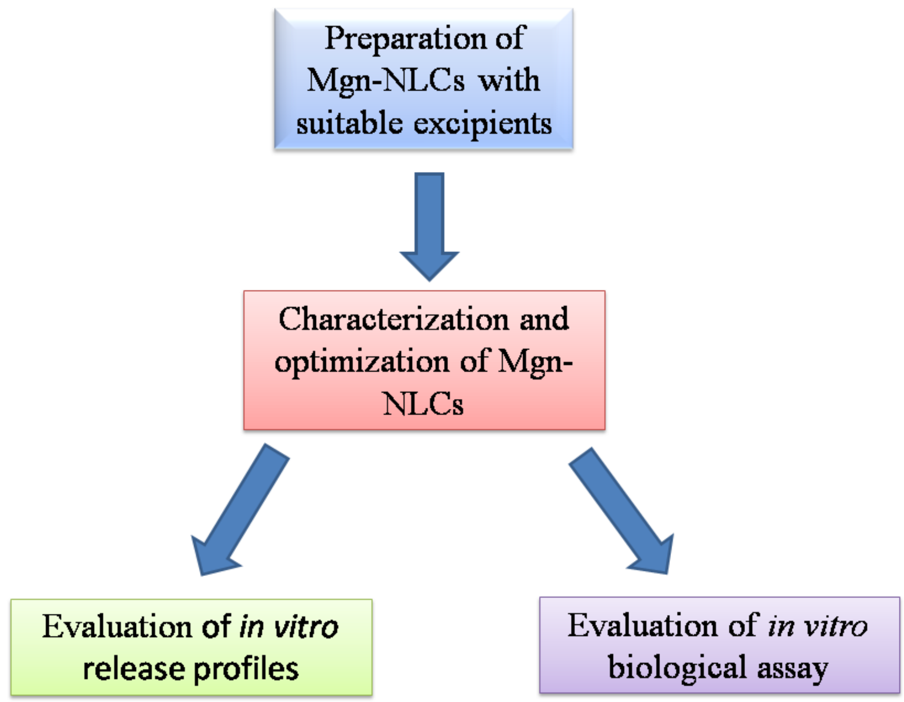

Figure 3.1. Plan of work, schematic representation

Chapter 4

Materials and Methods

Contents

4. Materials and Methods

4.1. Materials

Mgn (MW 422.3) was purchased from Sigma-Aldrich, India, beeswax was purchased from Unicorn Petroleum Industries Pvt. Ltd., olive oil was purchased from Bertolli, PVA was purchased from HiMedia Laboratories Pvt. Ltd. Ethanol and all other solvents of analytical grade were purchased from Merck Life Sciences Private Limited, India. FITC was purchased from Sigma-Aldrich, St. Louis, USA. The MCF-7 and MDA-MB-231 cells were procured from National Centre for Cell Science, Pune, India.

4.2. Methods

4.2.1. Determination of absorbance maxima of Mgn

1 mg of Mgn is accurately weighed and dissolved in 5 ml ethanol-water (1:1) to make an Mgn solution of concentration 200 µg/ml. This solution was used to determine the λ_{max} of Mgn after appropriate dilution using a UV-visible spectrophotometer (Intech-295, India), at the scanning range of 200-400 nm against blank.

4.2.2. Plotting of standard curve of Mgn

Mgn was dissolved in ethanol-water (1:1) to obtain a stock solution of concentration 100 µg/ml. Aliquots were taken from this stock solution and serial dilution of Mgn was done with concentrations ranging from 1-8 µg/ml diluting with the same solvent. The absorbances of these concentrations were measured using a UV-visible spectrophotometer (Model Intech-295, India) at the λ_{max} of Mgn to generate a standard curve of calibration. Ethanol-water (1:1) was used as a blank to adjust the values of absorbance. The readings were taken in triplicate.

For standard curve in phosphate buffer solution (PBS), Mgn was dissolved in PBS (pH 7.4) to obtain a stock solution of concentration 100 µg/ml. Aliquots were taken from this stock solution and serial dilution of Mgn is done with concentrations ranging from 1-16 µg/ml diluting with the same solvent. The absorbances of these concentrations were measured using a UV-visible spectrophotometer (Model Intech-295, India) at the λ_{max} of Mgn to generate a standard curve of calibration. PBS (pH 7.4) was used as a blank to adjust the values of absorbances. The readings were taken in triplicate.

4.2.3. Preparation of Mgn-NLCs

The high-speed stirring and ultrasonication method was used to prepare Mgn-NLCs with slight modifications (Das and Chaudhury, 2011; AkhoondZardini et al., 2018; Duong et al., 2020). Beeswax (solid lipid) and olive oil (liquid lipid) were first combined in a glass container dissolved in the acetone-ethanol mixture (1:1). The lipids were then heated at 75°C (above the melting point of solid lipid) while being continuously stirred to homogeneously mix them. To completely dissolve the drug Mgn, it was added to the mixture and thoroughly stirred. PVA (surfactant) was dissolved in water (1.5 % w/v) and heated to 75 °C in a different container. The heated aqueous surfactant solution (aqueous phase) was then added to the drug-containing molten lipids (oil phase) dropwise with continuous stirring. The solution was then stirred at a high speed with a magnetic stirrer (REMI® model no. 2-ML) to apply a high shear force to formulate an emulsion or pre-emulsion for at least 1 hour. This pre-emulsion is further subjected to ultra-sonication by using a probe sonicator (LABSONIC®M model no. BBI- 8535027) to break down the larger oil droplets into nanosized lipid droplets containing Mgn. The dispersion is then cooled to room temperature for solidifying the nanosized lipid droplets. The resultant dispersion was then centrifuged (Sigma 3-18KS) at 15000 rpm for 20 minutes and washed with distilled water twice. The pellet collected was then freeze-dried using a lyophilizer (ScanVacCoolSafe Basic) for 48 hours after suitable pre-freezing, and stored at 4 ± 1°C temperature. Blank NLCs were also prepared following a similar protocol. The overall formulation protocol has been depicted in Figure 4.1. The NLCs were prepared by varying the beeswax-olive oil ratio and optimized based on test results during characterization studies (Table 4.1). Fluorescent NLCs were prepared by replacing Mgn with FITC.

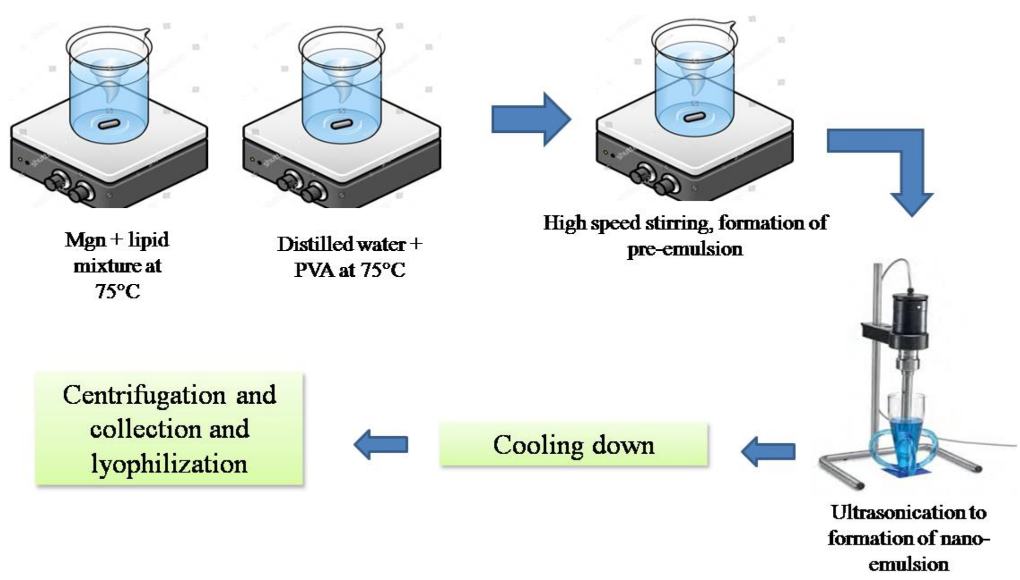

Figure 4.1. Formulation protocol of Mgn-NLCs

Table 4.1. Formulations with varying solid lipid-liquid lipid ratios for formulating Mgn-NLCs

Formulation codes	Solid lipid (mg)	Liquid lipid (mg)	Mgn (mg)
F1	45	5	2.5
F2	35	15	2.5
F3	30	20	2.5

4.2.4. Physico-chemical compatibility studies

4.2.4.1. Evaluation of drug excipient interaction by FTIR spectroscopy

In the FTIR spectroscopic study, all samples, such as Mgn, Beeswax, PVA, the physical mixture of Mgn with the excipients, blank NLCs and Mgn-NLCs were powdered properly for scanning in FTIR spectrophotometer (IR-Prestige-21 Shimadzu, Japan) to understand the possible chemical interactions occurring between the drug and other excipients (Kenechukwu et al., 2022). Each of the samples was crushed using KBr to form pellets and was scanned at 400-4000 cm^{-1}.

4.2.4.2. Crystallinity evaluation by powder XRD analyses

XRD patterns of Mgn, Beeswax, PVA, the physical mixture of Mgn with the excipients, blank NLCs and Mgn-NLCs were measured in an X-ray powder diffractometer (XRD-2000, Rigaku, Japan). The measurements were performed in the 5°-70° 2θ using CuKα radiation (45 kV, 40 mA) as the X-ray source and the rate of scanning was 1°/min to understand the possible chemical interactions occurring between the drug and lipid matrix.

4.2.5. Characterization of prepared NLCs

4.2.5.1. Yield, drug loading (DL) and entrapment efficiency (EE) of NLCs

The yield of NLCs is determined by weighing the resultant formulation and yield percentage is calculated by the equation,

$$\% \text{ Yield} = \frac{\text{Amount of drug and lipid used (mg)}}{\text{Amount of NLCs obtained (mg)}} \times 100$$

NLCs' effectiveness at encapsulating was assessed. NLCs were dissolved in ethanol-water (1:1) with a concentration of 1 mg/ml in centrifuge tubes, and the tubes were assembled in a centrifuge (Sigma 3-18KS). The centrifuge was run for 30 minutes at an optimal speed of 4000 rpm.1 ml of the supernatant phase was collected; ethanol-water (1:1) was used to dilute it 100 times. Using a UV-VIS spectrophotometer (Intech-295, India), the absorbance values of the dilutions were collected at a specified wavelength of maximum absorption (257 nm).

Using the conventional Beer-Lambert's plot for Mgn in distilled water, the amounts of drug encapsulated in the NLCs were estimated and the EE percent was calculated (Kenechukwu et al., 2022).

$$\% \text{ EE} = \frac{\text{Amount of drug present in NLCs (mg)}}{\text{Amount of drug that was given in formulation (mg)}} \times 100$$

DL is defined as the ratio of the amount of the drug that is entrapped by the lipid to the total amount of lipids utilised in the formulation (Kenechukwu et al., 2022).

$$\% \text{ DL} = \frac{\text{Amount of drug present in NLCs (mg)}}{\text{Amount of lipid used to prepare NLCs (mg)}} \times 100$$

4.2.5.2. Particle size and surface charge measurements

A zetasizer Nano-ZS90 was used to measure the NLCs' particle size and particle density index (PDI) (Malvern Instruments, Worcester, UK). We compared the 9Z-carotene high-loaded NLCs' appearances at dilutions of 1, 10, 100, and 1000 times. To assess the particle size and PDI, the original preparation was diluted by 1000 times in deionized water. The intensity distribution's grain size was assessed. For the purpose of gathering PDI and particle diameter data, three measurements were made (Yang et al., 2020). This sample was also used for measurement of zeta potential at 25 °C temperature using Malvern Zetasizer Nano ZS (Malvern Instruments, Worcester, UK) (Yang et al., 2020).

4.2.5.3. SEM

SEM (JEOL-JSM-6 360, Japan) was used to analyze the formulations' morphological properties at various magnifications. One sample drop was applied on a slide, and any extra liquid was allowed to dry at room temperature. The slide was coated with gold using a sputter coater (Model JFC-1100, JEOL, Japan) under the vacuum for 10 minutes before being examined at 5 kV. The specimen holder was connected to the slide using double-coated adhesive tape (Kenechukwu et al., 2022).

4.2.5.4. TEM

TEM was used to determine the morphological traits of the Mgn-NLCs. To dilute the NLCs by a factor of 1,000, deionized water was added. On copper grids that were coated with carbon, one drop of the diluted sample was applied, and it was allowed to air dry. Using an FEI Tecnai G2 F20 S-TWIN TEM at 200 kV, the sample was viewed after being stained with phosphotungstic acid (Yang et al., 2020).

4.2.6. *In vitro* drug release study

The release media was 500 ml of freshly made PBS (0.1 M, pH 7.4) kept at 37 °C using a thermostatic water bath. Prior to the start of the release experiment, the polycarbonate dialysis membrane (Dialysis Membrane-60, HIMEDIA) that served as a release barrier was pre-treated by soaking in the release medium for 24 hours. Each time, 2 ml of the drug-loaded NLCs were placed in the dialysis membrane, tied off with thermo-resistant thread, and then submerged in the release medium while being stirred by a paddle rotating at 100 rpm. At regular intervals of time (1, 2, 3, 6, 12,24, 48, 72, 96, 120, 144, 168, 192 h), to maintain a sink condition, 5 ml of the release media were removed and replaced with an equivalent volume of the medium. The removed medium was then filtered using a millipore filter (Millipore, Delhi, India) and spectrophotometrically examined (Intech-295, India). The typical Beer's plot for Mgn in PBS was used to calculate the amount of medication released at each time interval. Plotting against time showed the cumulative Mgn release percentage (Kenechukwu et al., 2022).

4.2.7. *In vitro* pharmacokinetic modelling

In vitro drug release patterns are usually classified using different mathematical models representing release kinetics. The accurate pharmacokinetic modelling can be determined by comparing the nature of the curve with the existing mathematical models. Different mathematical models were used to predict the manner of drug release from formulation. Experimental data obtained from *in vitro* release study were fitted to various kinetic equations viz. zero order, first order, square root of mass, Higuchi, Hixson-Crowell, and Korsmeyer-Peppas models to investigate the mechanistic pattern of drug release from lipid matrix of Mgn-NLCs (Mircioiu et al., 2019).

4.2.8. Stability study

Freeze-dried NPs were kept at 4 ± 1 °C for 90 days and scrutinized for the diameter of particles, distribution of particle size, and zeta potential according to the methods described by Gaonkar and colleagues (2017).

4.3. *In vitro* anticancer assays

Against two breast cancer cell lines, such as MDA-MB-231 and MCF-7 *in vitro* the metabolic effects of Mgn-NLCs and free Mgn were evaluated employing breast cancer cells. The effect on metabolic activity on a non-cancer cell line, the NKE cell line was also included in this study to check the tumor cell-specific activity of the free drug and drug-loaded NLCs. Briefly, the cells (~2000 cells/well) were plated to a 384-well microplate and incubated at 5% CO_2 and 37 °C for 24 h (Das et al., 2019). The cell monolayers were treated with Mgn-NLCs and free Mgn at different concentrations and incubated under the same condition for 24 h. Then, 5 μL resazurin (60 μM) was added to each well and incubated for 2 h. Fluorescence was measured at $\lambda_{excitation}/\lambda_{emission}$ 535/590 nm.

4.4. Hoechst Staining

Hoechst staining was executed to perceive *in vitro* cytotoxicity under the fluorescence microscope. In brief, the cells (~2000 cells/well) were plated to a 384-well microplate and incubated at 5% CO_2 and 37 °C for 24 h (Das et al., 2019). The cell monolayers were treated with Mgn-NLCs and free Mgn of same concentrations (IC_{50} of Mgn) and incubated under the same condition for 24 h. The, the cells were fixed with 4 % of paraformaldehyde in phosphate buffer saline (pH 7.4) for 20 min. The cells were subsequently stained with Hoechst 33258 (5 μg/mL in PBS) for 20 min and washed with cold PBS. Fluorescent nuclei and nuclear patterns were noted. A couple of sets of free Mgn-treated groups and a couple of untreated (controls) for both breast cancer cells were kept for the comparison.

Chapter 5

Results and Discussion

Contents

5. Results and discussions

5.1. Absorbance maxima of Mgn

Absorbance maxima is the highest absorbance value in the absorbance versus wavelength plot; the lowest possible concentration of a compound can be detected as it is the most accurate place to measure because of small errors in setting the wavelength in the spectrophotometer. The λ_{max} value was found to be 257 nm (Figure 5.1). So, the absorbance of Mgn solutions in different solvents should be measured at 257 nm to get absorbance values with minimum errors.

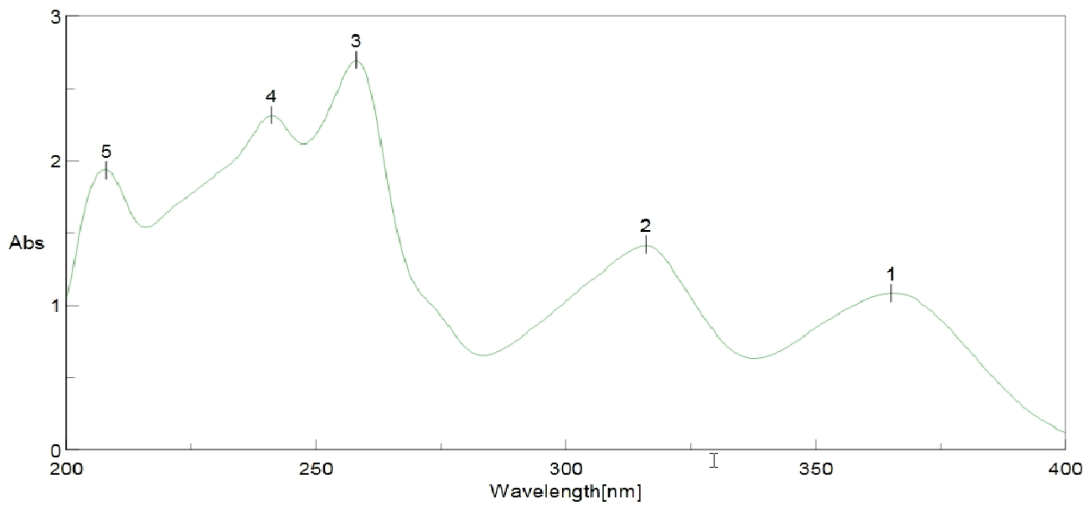

Figure 5.1. λ_{max} of Mgn

5.2. Standard curve of Mgn

A standard curve is based on the principle of Beer-Lambert's law, which states that the quantity of light absorbed by a substance dissolved in a fully transmitting solvent is directly proportional to the concentration of the substance and the path length of the light passing through the solution (Baker et al., 2014). Plotting the standard curve of a compound dissolved in a certain solvent helps in the determination of the unknown concentration of the solution of that compound. The standard curve of Mgn in ethanol-water (1:1) follows linearity (Figure 5.2) exhibiting an R^2 value of 0.995. This equation shows that the increase in the concentration of an ethanol-water solution of Mgn is directly proportional to the increase of absorbance values. The standard curve of Mgn in PBS (pH 7.4) follows linearity (Figure 5.3) and bears the equation: $y = 0.059x – 0.011$ and has an R^2 value of 0.997. This equation shows that the increase in the concentration of PBS solution of Mgn is directly proportional to the increase of absorbance values.

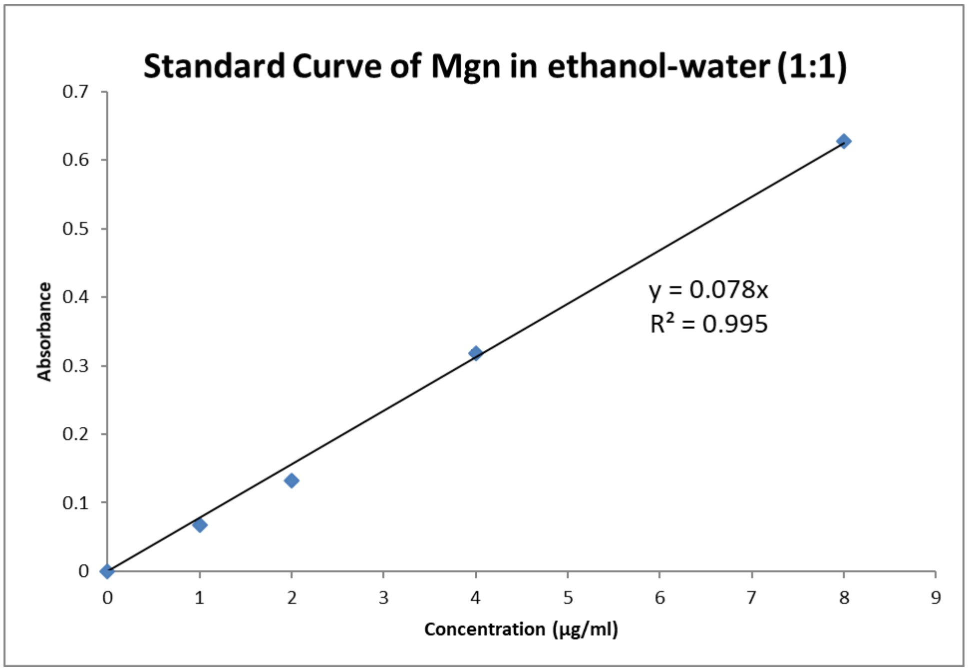

Figure 5.2. Standard curve of Mgn in ethanol-water (1:1)

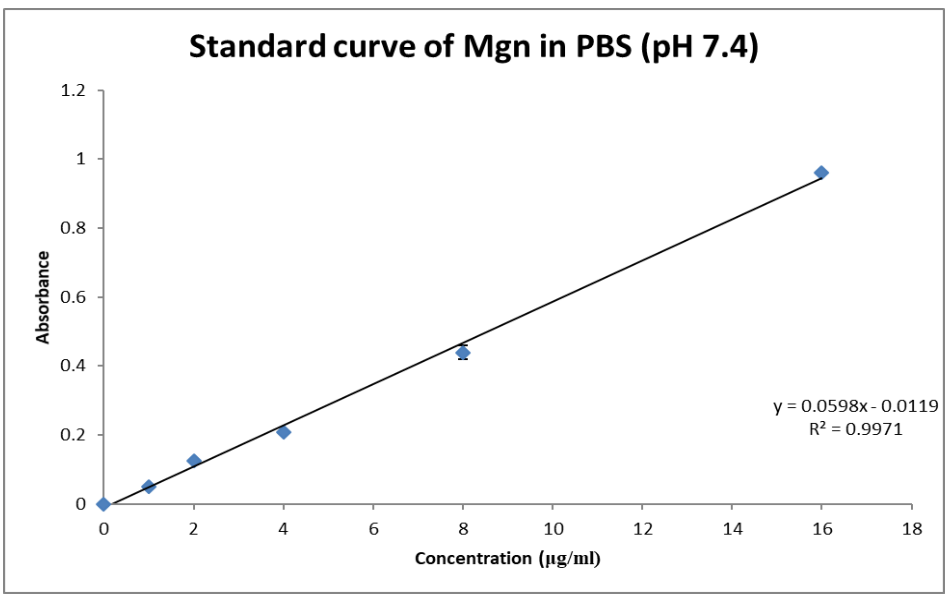

Figure 5.3. Standard curve of Mgn in PBS (pH 7.4)

5.3. Yield, DL and EE

The amount of Mgn loaded in the NLCs was determined by spectroscopic measurements at 257 nm. DL amounts and EE of various Mgn-NLCs prepared by varying the solid lipid-liquid lipid were measured. The highest yield of NLCs was reported to be 85.56 ± 3.7%, the highest EE was detected as 91.76 ± 4.9 %, and the highest DL content of Mgn in Mgn-NLCs was detected as 5.1 ± 0.37 %. In a study with hydrochlorthiazide-loaded NLCs, the formulated

NLCs which had EE of around 90% were suitable for further therapeutic studies (Mura et al., 2021). Another study that reported >95% of EE and >5% of DL for sucupira oil-loaded NLCs showed effective therapeutic results in *in vitro* and *in vivo* studies (Vieira et al., 2020). Based on these reports the formulated Mgn-NLCs can be used for therapeutic approaches. So, it can be said that Mgn was encapsulated into NLCs with a relatively high DL capacity and EE, which might be due to unstable crystal structures that were incorporated by mixing solid and liquid lipid. Yield, DL, and EE are tabulated and compared between different formulations formulated with varying solid lipid-liquid lipid ratios in Table 5.1 and Figure 5.4. Comparing the yield (Figure 5.4A), DL (Figure 5.4B) and EE % (Figure 5.4C) with varying solid lipid-liquid lipid ratios (9:1, 7:3, and 6:4), it was observed that mixing the lipids in the ratio 7:3 yielded maximum NLCs with maximum drug entrapment.

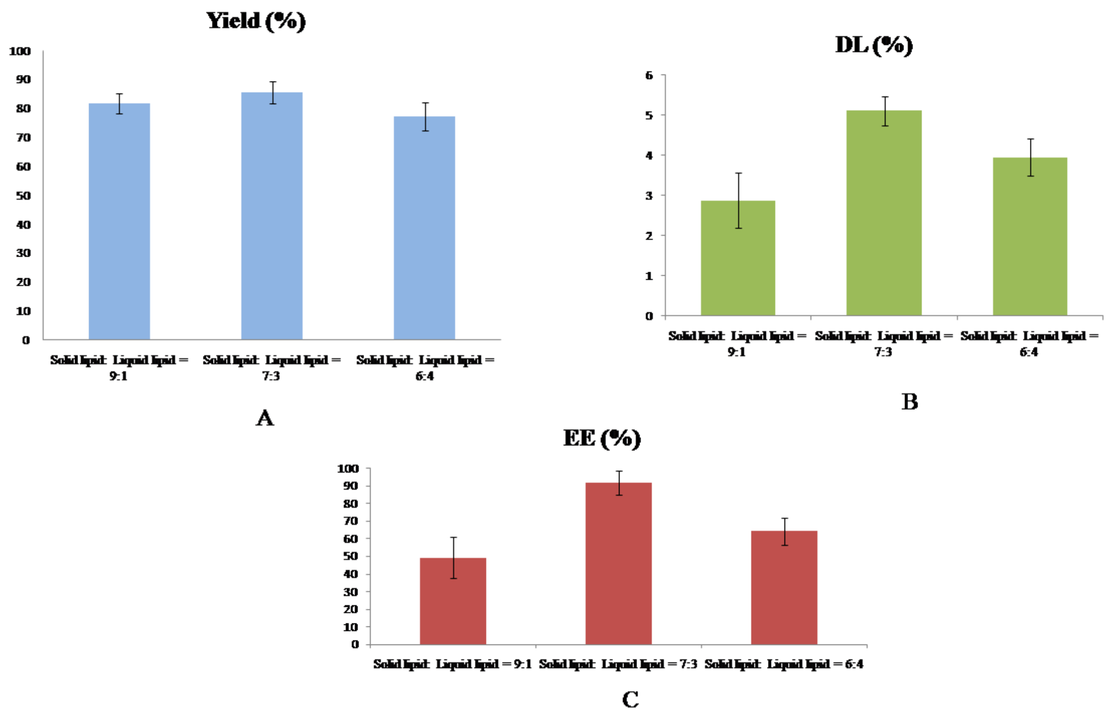

Figure 5.4. Comparison between yield (A), DL (B), and EE (C) in different solid lipid-liquid lipid ratios

5.4. Particle size and size distribution

DLS study also analyzes the size of NLCs. This DLS study reveals that the average diameter of NLCs to be 306.6 ± 22.5 nm (Figure 5.5) and PDI was found to be 0.311. In microscopic methods the size parameters are determined exactly from the original surface of the particle whereas in DLS the light beam scatters from the stagnant solvent layer adhered to its surface, thus the size determined includes the thin film of solvent. Particle size of formulations with different solid lipid-liquid lipid ratios were compared in Table 5.1.

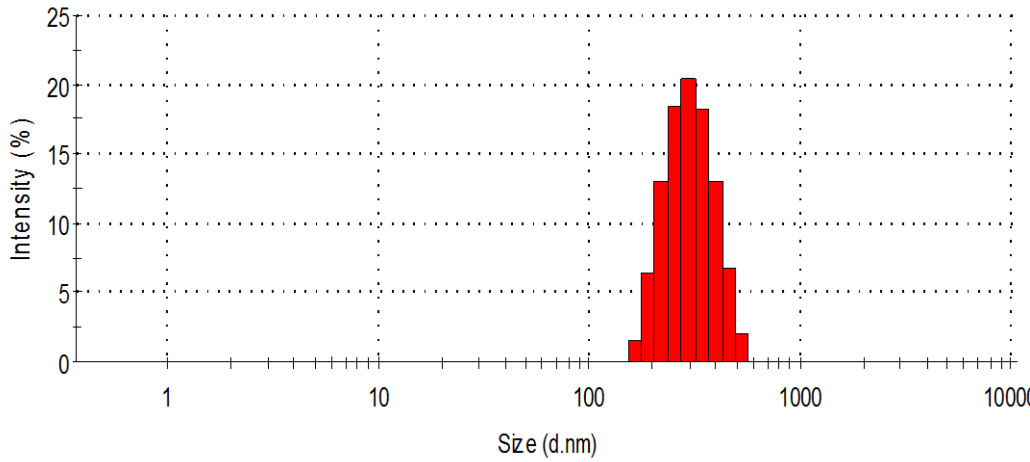

Figure 5.5. Particle size distribution pattern of Mgn-NLCs

5.5. Surface Charge

Zeta-potential value of Mgn-NLCs was found to be -10.1 ± 4.70 mV (Figure 5.6). NLCs having zeta potential between -10 and +10 mV are reportedly electronically inert in nature, on the other hand, zeta potential values of greater than +30 mV or less than -30 mV are reported as strongly cationic and strongly anionic, respectively. As maximum cellular membranes are negatively charged, NLCs with negative zeta potential value would easily permeate cellular membranes and would not cause toxicity (Clogston and Patri, 2011). The surface charge of different formulations with variable solid lipid-liquid lipid ratio has been compared in Table 5.1. Considering the reports from the literature mentioned here, it can be predicted that the developed Mgn-NLCs would be favourable for administration.

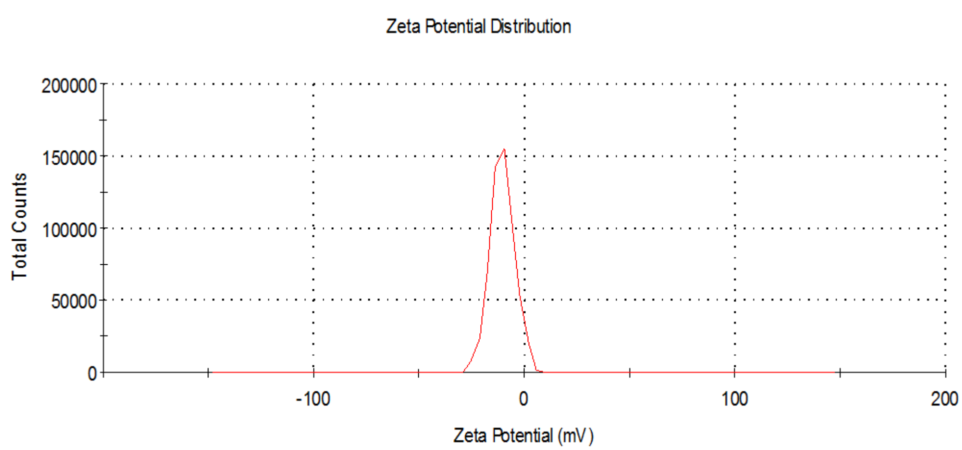

Figure 5.6. Zeta potential distribution profile of Mgn-NLCs

Table 5.1. Particle size, surface charge, yield, DL, and EE %s of different formulations

Formulation Codes	Particle size (nm)	Surface Charge (mV)	Yield (%)	DL (%)	EE (%)
F1	296.5 ± 32.5	-15.1 ± 3.57	81.67 ± 3.5	2.87 ± 0.69	49.22 ± 11.83
F2	306.6 ± 22.5	-10.1 ± 4.70	85.56 ± 3.7	5.10 ± 0.37	91.76 ± 6.64
F3	340.9 ± 17.9	-8.1 ± 2.81	77.31 ± 4.8	3.95 ± 0.46	64.13 ± 7.46

Based on the above results, formulation F2 has been optimized for *in vitro* experiments.

5.6. FTIR analyses

FTIR studies provide information about the stability of the formulation, as well as the interaction between drugs and the excipients in the formulation (Gaonkar et al., 2017). Each compound has its own characteristic FTIR peaks due to the presence of different covalent bonds. According to vibrational spectroscopy, each bond has its own vibrational energy, which is unique, and thus helps to distinguish one component from the other (Zhao et al., 2022). In this study, FTIR spectra were recorded for Mgn, beeswax, PVA, a physical mixture of Mgn, beeswax and PVA, blank NLCs and Mgn-NLCs (Figure 5.7), where the transmittance is plotted on the y axis and the wave number is on the x-axis. From these FTIR results it can be seen, that the spectra showed characteristic peaks of Mgn at 3365 cm^{-1} is due to the presence of secondary OH- bonds, peak at 3184 cm^{-1} showed C-H antisymmetric stretching, peak at 2889 cm^{-1}, 1649 cm^{-1}, 1492 cm^{-1}, and 1095 cm^{-1} indicated presence of C-H symmetric stretching, C-O stretching, CH-CH bending and C-O bond. A peak at 1031 cm^{-1} showed the presence of C-C stretching in the structure of Mgn (Figure 5.7 C). The FTIR spectrum of beeswax revealed the characteristic peak at 2916 cm^{-1} and 2848 cm^{-1} for symmetric and asymmetric stretching for C-H bonds, a peak at 1463 cm^{-1} was observed for the C-H bending or scissoring and C-H rocking was demarketed by the peak which was observed at 719 cm^{-1}(Figure 5.7 B). In the FTIR spectrum of PVA, the peak shown at 3259 cm^{-1} indicated the presence of -OH stretching, the peak at 2922 cm^{-1} indicated the asymmetric stretching of $-CH_2$, the peak at 1720 cm^{-1} indicated C=O carbonyl stretching, the peak at 1460 cm^{-1} indicated $–CH_2$ bending, and the peak at 1039 cm^{-1} indicated C-O stretching (Figure 5.7 A). Most of the characteristic peaks of Mgn, beeswax, and PVA appeared in the FTIR spectrum of the physical mixture without any major change in peak position or intensity (Figure 5.7 D) and in the blank NLCs, all except Mgn's peaks are present unaffectedly (Figure 5.7 E). Similarly, in Mgn-NLCs, the presence of the characteristic peaks of the Mgn and excipients indicates the presence of Mgn in pure form without any chemical interactions with the wax or lipid material (beeswax) or with the surfactant (PVA) (Figure 5.7 F).

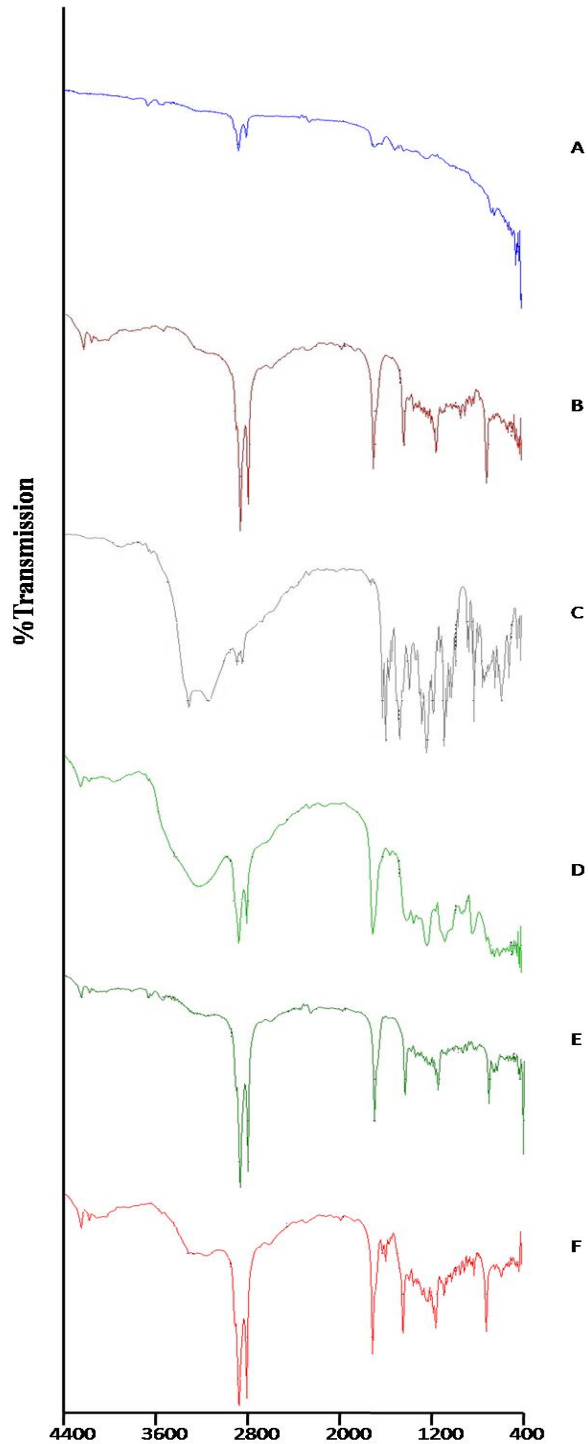

Figure 5.7. FTIR spectra of PVA (A), beeswax (B), Mgn (C), physical mixture (D), Blank NLCs (E), Mgn-NLCs (F)

5.7. Crystallinity evaluation by XRD

XRD analysis detects the presence of crystalline property of samples; amorphous materials, like polymers, do not produce any sharp peaks, whereas sharp peaks with high intensity are found in crystalline materials (Bunaciu et al., 2015). XRD patterns of Mgn, beeswax, PVA, their physical mixture, blank NLCs, and Mgn-NLCs are shown in Figure 5.8, where the X-axis represents 2θ values and the y-axis represents intensity (cps). The peaks for free Mgn found to be free of distortion and have high intensity, which indicates that Mgn is crystalline in nature (Figure 5.8 C). The absence of sharp peaks in the XRD of beeswax confirmed its amorphous nature (Figure 5.8 B), the crystalline nature of PVA was also confirmed by the presence of sharp high intensity peaks (Figure 5.8 A). Minor reference peaks could be lost in the background noise, so it may be acceptable if they are not observed (Bunaciu et al., 2015). The physical mixture of Mgn, beeswax and PVA exhibited a number of distinct peaks; the position of peaks were almost the same compared to pure samples suggesting minimum to no interaction between the components (Figure 5.8 D). The disappearance of distinct peaks in blank NLCs (Figure 5.8 E) and Mgn-NLCs suggested the conversion of crystalline to amorphous state during NLC formulation (Figure 5.8 E). The highest intensity values of the components are mentioned in Table 5.1.

Table 5.2. Highest intensity values of different components

Samples	Highest intensity
Free Mgn	9968
Beeswax	820
PVA	874
Physical mixture	9940
Mgn-NLCs	843

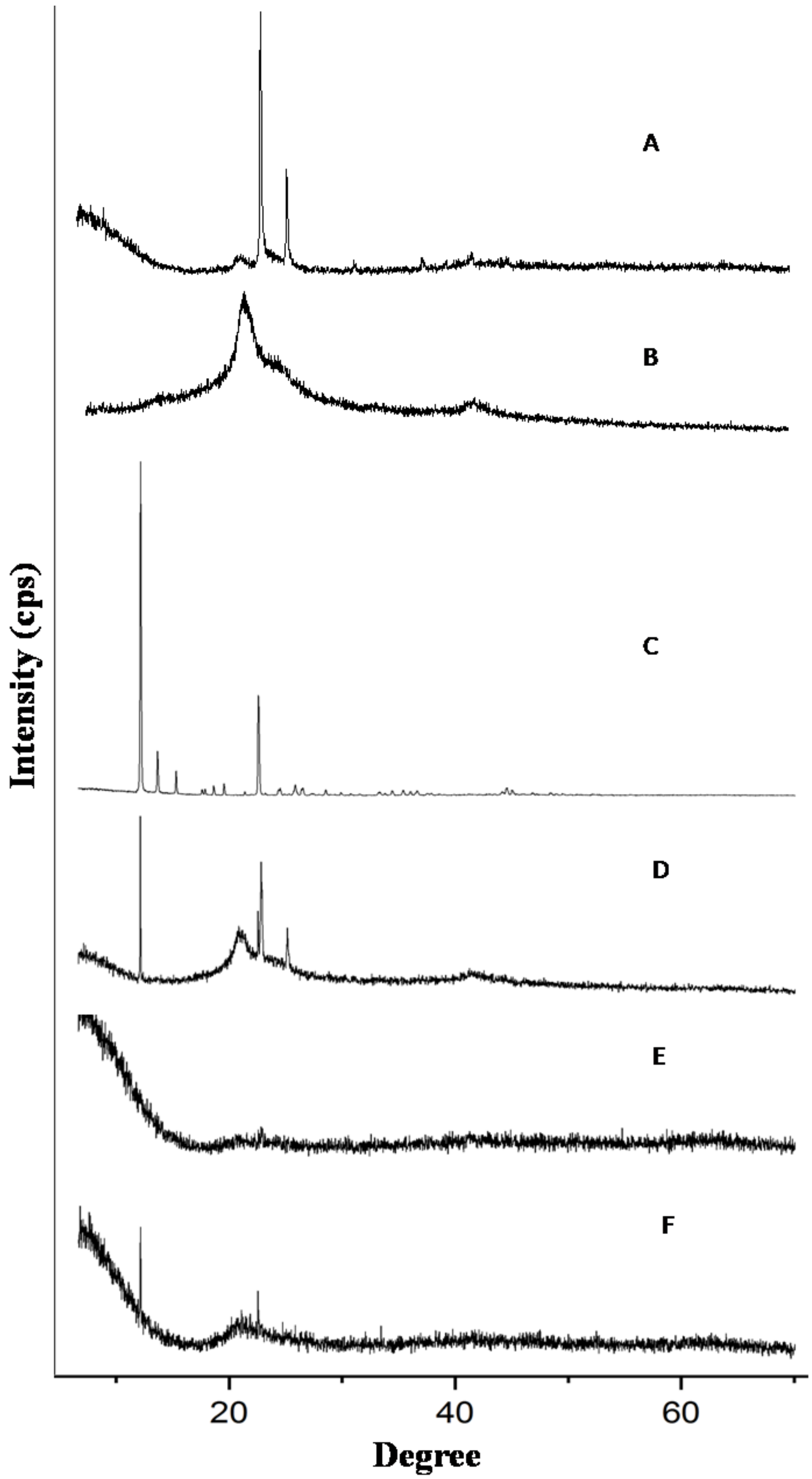

Figure 5.8. XRD of PVA (A), beeswax (B), Mgn (C), physical mixture (D), blank NLCs (E) and Mgn-NLCs (F)

5.8. SEM

SEM images showed spherical particulate distribution and smooth surface morphology with particle size lying around 300 nm (Figure 5.9 A). There was no visible aggregation of the particles. The size range it lies in is smaller but comparable to size data obtained from DLS. According to several reports, NLCs with similar parameters can be used for further studies and applications (Barbosa et al., 2016; Shirazi et al., 2021).

5.9. TEM

The TEM image showed a discrete spherical outline and monodispersed size distribution of NLCs and measured its size around 300 nm (Figure 5.9 B). There was no visible aggregation of the particles. The size range it lies in is smaller but comparable to size data obtained from DLS and SEM. Similar data was reported by several literature, hence can be considered as acceptable (Barbosaet al., 2016; Shirazi et al., 2021). So, the size of Mgn-NLCs determined by TEM analysis can be considered as acceptable size and can be further used for therapeutic approaches.

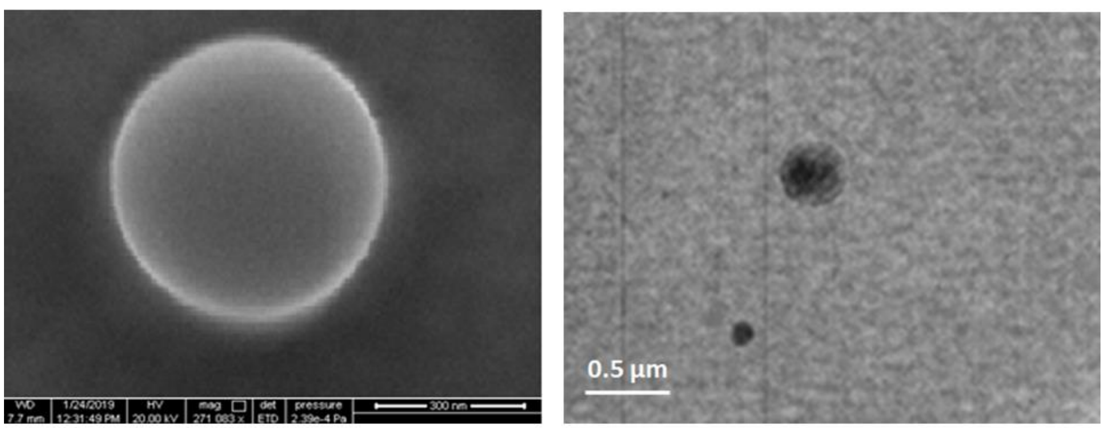

A **B**

Figure 5.9 SEM images of Mgn-NLCs (A), TEM images of Mgn-NLCs (B)

5.10. *In vitro* drug release study

Initial release was 20.1% within first 3 h (Figure 5.10). Initial release with high % of drug release may take place if some unincorporated drug particles were loosely attached to lipid surface. The release was moderate up to 24 h; this was followed by a slower sustained release. The property of long duration release of drug makes NLCs act like drug depot, which exhibits prolonged release kinetics and long persistence at the target site (Qamar et al., 2019). Around 88.01% of Mgn was released from NLCs over the period of 8 days. *In vitro* drug release from NLCs usually occurs in 2 steps. At first, the burst release takes place, due to the adhesion of drug substances on the NLCs surfaces and then prolonged release starts (Qamar et al., 2019).

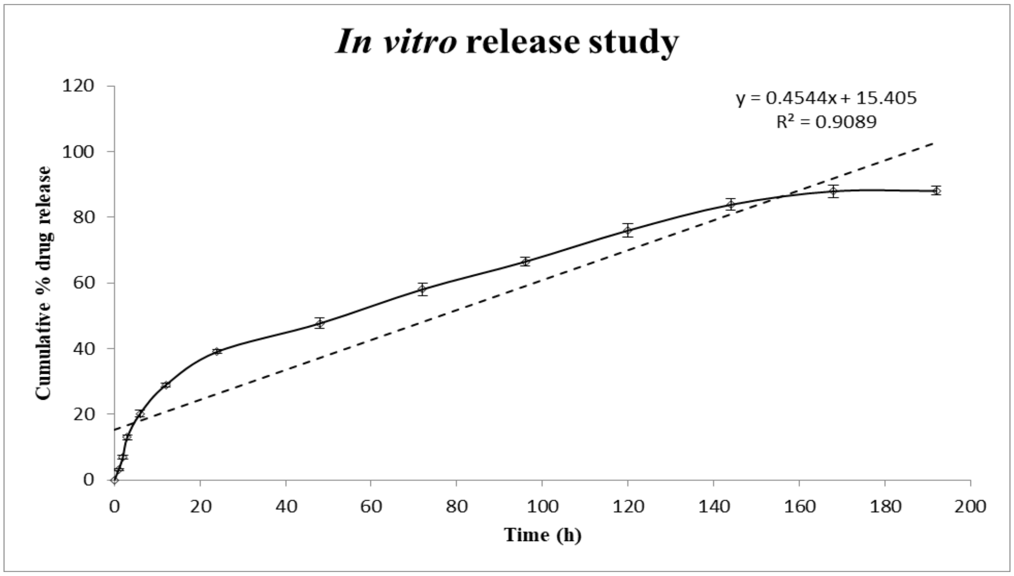

Figure 5.10. *In vitro* release of Mgn from optimized NLCs

5.11. *In vitro* pharmacokinetic modeling

Drug release was analyzed by comparing with various drug release pharmacokinetic models (Figure 5.11). Korsmeyer-Peppas release plot (Figure 5.11 A), First order release plot (Figure 5.11 B), Higuchi plot (Figure 5.11 C) and Hixson-Crowell plot (Figure 5.11 D) were determined from the data obtained from *in vitro* release study to determine the pharmacokinetic model of Mgn-NLCs. As depicted in table 5.3, release profile was best fitted with Higuchi model.based on regression coefficient (R^2) values. Korsmeyer-Peppas release exponent value of 0.564 suggests non-Fickian diffusion mechanism of drug release (Dash et al., 2010).

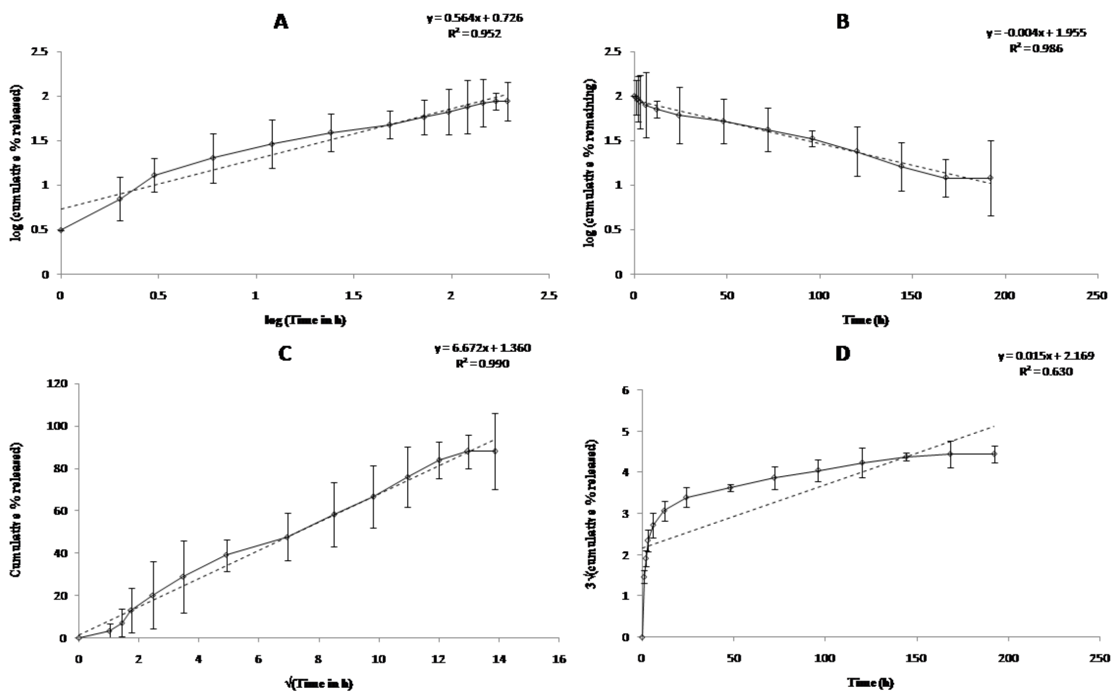

Figure 5.11. Korsmeyer-Peppas release (A), first order release (B), Higuchi release (C) and Hixson-Crowell release (D) models for optimized Mgn-NLCs

Table 5.3. Equations and regression coefficients of different pharmacokinetic models

Pharmacokinetic Mode	Equations	Regression Coefficients
Zero order	y=0.4544x + 15.405	0.9089
Korsmeyer-Peppas release	y= 0.564x + 0.726	0.952
First order release	y= 0.004x + 1.955	0.986
Higuchi release	y= 6.672x + 1.360	0.990
Hixson-Crowell release	y= 0.015x + 2.169	0.630

5.12. Stability study

Prepared Mgn-NLCs stored at 4 ± 1 ^{o}C did not show any change with respect to the diameter of particles, distribution of particle size, and zeta potential after 90 days confirming the stability of developed NLCs.

5.13. *In vitro* anticancer assays

To find out the effects of Mgn-NLCs on the metabolic activities on MCF-7 and MDA-MB-231 cells resazurin-based bioassay has been performed (Figure 5.12). Mgn-NLCs exhibited a dose-dependent reduction of metabolic activities in both the breast cancer cells without affecting normal cells suggesting cancer cell-specific inhibitory effect on the metabolic activity. However, the effect of Mgn-NLCs is more pronounced than that of free Mgn depicting the therapeutic potential of the formulation over free drug.

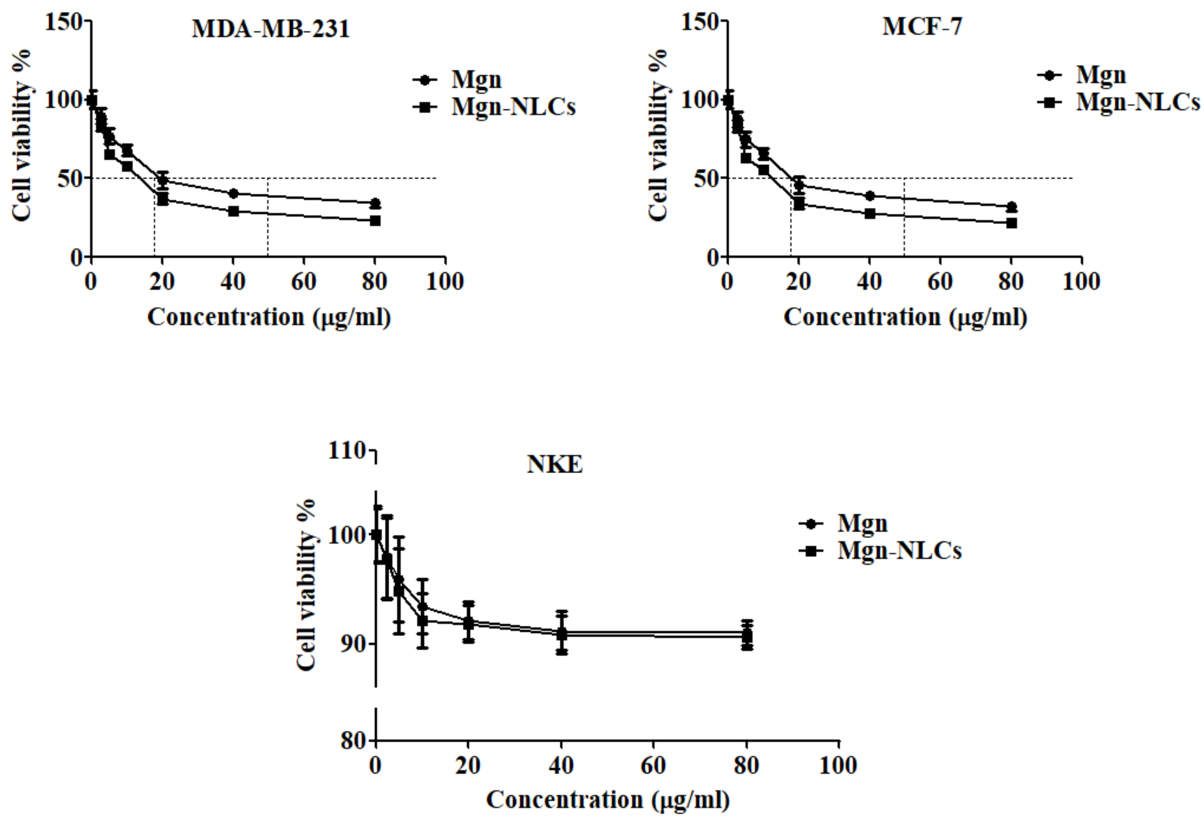

Figure 5.12. Effect of Mgn-NLCs and Mgn on the metabolic activity of MCF-7, MDA-MB-231, and NKE cells.

5.14. Hoechst Staining

Hoechst nuclear staining was executed to envisage the nuclear score after the treatment with Mgn-NLCs and Mgn on MCF-7 and MDA-MB-231 cells (Figure 5.13). Hoechst staining of the breast cancer cells treated with Mgn-NLCs and free Mgn showed a significantly low number of viable cells with unambiguous configurations of morphological changes including shrinkage, abridgement, and fragmentation, which clearly suggests the induction of apoptosis to the breast cancer cells as compared to untreated control.

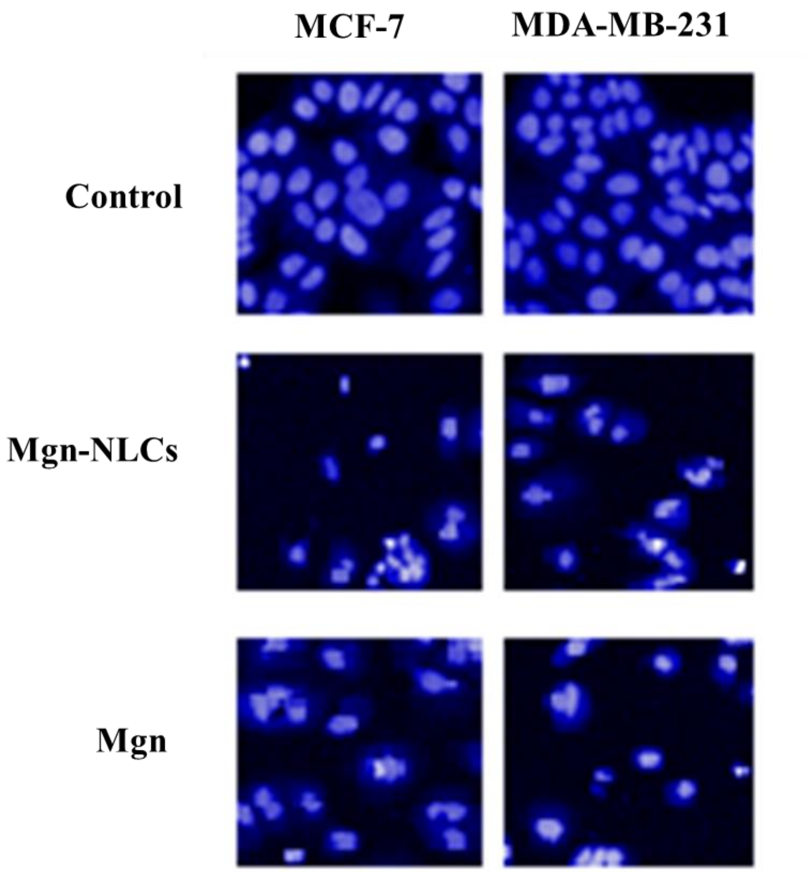

Figure 5.13. Effect of Mgn-NLCs and Mgn on the Hoechst nuclear staining to MCF-7 and MDA-MB-231 cells.

However, the effect of Mgn-NLCs treatment is more pronounced than that of Mgn-treated breast cancer cells evidenced by nuclear counts and patterns as revealed through Hoechst staining.

Chapter 6

Conclusion

6. Conclusion

Mgn possesses antidiabetic, anticancer, neuroprotective, cardioprotective, antioxidant, anti-inflammatory, antiviral, antimicrobial, antiallergic and hepatoprotective properties. However, due to very low solubility and permeability, Mgn exhibits low bioavailability. On reviewing more reports, it has been found that therapeutically active compounds can be delivered encapsulated in NLCs to enhance their bioavailability. The Mgn-loaded NLCs were prepared using beeswax and olive oil as lipids and PVA as an emulsifier by the high-speed stirring-ultrasonication method. The results of physicochemical characterization of Mgn, beeswax, olive oil, PVA, physical mixture of Mgn, beeswax, olive oil and PVA, and Mgn-NLCs showed that Mgn is compatible with the excipients used to prepare Mgn-NLCs and its physicochemical properties were not affected. The yield of NPs, the drug loading and the entrapment efficiency of the drug in NLCs were found to be significant. The mean particle size and surface charge of Mgn-NLCs were found to be favourable in drug delivery and cell membrane penetration. The *in-vitro* drug release study showed a sustained release of entrapped drug over a period of 8 days. The physical parameters of the formulation do not change with prolonged storage indicating their stability. The formulation also exhibited a significant improvement of the anti-cancer effect on MCF-7 and MDA-MB-231 cells *in vitro* as compared to free Mgn. Therefore, it may be claimed that Mgn-NLCs would be a potential formulation for subjecting to further pre-clinical studies to evaluate their therapeutic activities and efficacy over free Mgn.

References

References

Aghebati-Maleki A, Dolati S, Ahmadi M, Baghbanzhadeh A, Asadi M, Fotouhi A, Yousefi M, Aghebati-Maleki L. Nanoparticles and cancer therapy: Perspectives for application of nanoparticles in the treatment of cancers. J Cell Physiol. 2020;235(3):1962-1972. doi: 10.1002/jcp.29126.

Agrawal Y, Petkar KC, Sawant KK. Development, evaluation and clinical studies of Acitretin loaded nanostructured lipid carriers for topical treatment of psoriasis. Int J Pharm. 2010;401(1-2):93-102. doi: 10.1016/j.ijpharm.2010.09.007.

Ahmad A, Ahsan H. Lipid-based formulations in cosmeceuticals and biopharmaceuticals. Biomed. dermatol. 2020;4(1):1-0. doi: 10.1186/s41702-020-00062-9.

Akhoond Zardini A, Mohebbi M, Farhoosh R, Bolurian S. Production and characterization of nanostructured lipid carriers and solid lipid nanoparticles containing lycopene for food fortification. J Food Sci Technol. 2018;55(1):287-298. doi: 10.1007/s13197-017-2937-5.

Amasya G, Aksu B, Badilli U, Onay-Besikci A, Tarimci N. QbD guided early pharmaceutical development study: Production of lipid nanoparticles by high pressure homogenization for skin cancer treatment. Int J Pharm. 2019;563:110-121. doi: 10.1016/j.ijpharm.2019.03.056.

Andrade LN, Oliveira DML, Chaud MV, Alves TFR, Nery M, da Silva CF, Gonsalves JKC, Nunes RS, Corrêa CB, Amaral RG, Sanchez-Lopez E, Souto EB, Severino P. Praziquantel-Solid Lipid Nanoparticles Produced by Supercritical Carbon Dioxide Extraction: Physicochemical Characterization, Release Profile, and Cytotoxicity. Molecules. 2019;24(21):3881. doi: 10.3390/molecules24213881.

Attia MF, Anton N, Wallyn J, Omran Z, Vandamme TF. An overview of active and passive targeting strategies to improve the nanocarriers efficiency to tumour sites. J Pharm Pharmacol. 2019;71(8):1185-1198. doi: 10.1111/jphp.13098.

Baker WB, Parthasarathy AB, Busch DR, Mesquita RC, Greenberg JH, Yodh AG. Modified Beer-Lambert law for blood flow. Biomed Opt Express. 2014;5(11):4053-75. doi: 10.1364/BOE.5.004053.

Barbosa JP, Neves AR, Silva AM, Barbosa MA, Reis MS, Santos SG. Nanostructured lipid carriers loaded with resveratrol modulate human dendritic cells. Int J Nanomedicine. 2016;11:3501-16. doi: 10.2147/IJN.S108694.

Battaglia L, Muntoni E, Chirio D, Peira E, Annovazzi L, Schiffer D, Mellai M, Riganti C, Salaroglio IC, Lanotte M, Panciani P, Capucchio MT, Valazza A, Biasibetti E, Gallarate M. Solid lipid nanoparticles by coacervation loaded with a methotrexate prodrug: preliminary study for glioma treatment. Nanomedicine (Lond). 2017;12(6):639-656. doi: 10.2217/nnm-2016-0380.

Bayda, S., Adeel, M., Tuccinardi, T., Cordani, M., & Rizzolio, F. (2019). The History of Nanoscience and Nanotechnology: From Chemical–Physical Applications to Nanomedicine. Molecules, 2020;*25*(1), 112. doi: 10.3390/molecules25010112.

Begines B, Ortiz T, Pérez-Aranda M, Martínez G, Merinero M, Argüelles-Arias F, Alcudia A. Polymeric Nanoparticles for Drug Delivery: Recent Developments and Future Prospects. Nanomaterials (Basel). 2020;10(7):1403. doi: 10.3390/nano10071403.

Biswas T, Sen A, Roy R, Maji S, Maji HS. Isolation of mangiferin from flowering buds of Mangifera indica L and its evaluation of in vitro antibacterial activity. J Pharm Anal. 2015;4(3):49-56.

Bunaciu AA, Udriştioiu EG, Aboul-Enein HY. X-ray diffraction: instrumentation and applications. Crit Rev Anal Chem. 2015;45(4):289-99. doi: 10.1080/10408347.2014.949616.

Calva-Estrada SD, García O, Mendoza MR, Jiménez M. Characterization of O/W emulsions of carotenes in blackberry juice performed by ultrasound and high-pressure homogenization. J Dispers Sci Technol. 2018;39(2):181-9. doi: 10.1080/01932691.2017.1306783

Cano A, Sánchez-López E, Ettcheto M, López-Machado A, Espina M, Souto EB, Galindo R, Camins A, García ML, Turowski P. Current advances in the development of novel polymeric nanoparticles for the treatment of neurodegenerative diseases. Nanomedicine (Lond). 2020;15(12):1239-1261. doi: 10.2217/nnm-2019-0443.

Cao SJ, Xu S, Wang HM, Ling Y, Dong J, Xia RD, Sun XH. Nanoparticles: Oral Delivery for Protein and Peptide Drugs. AAPS PharmSciTech. 2019;20(5):190. doi: 10.1208/s12249-019-1325-z.

Caputo F, Clogston J, Calzolai L, Rösslein M, Prina-Mello A. Measuring particle size distribution of nanoparticle enabled medicinal products, the joint view of EUNCL and NCI-NCL. A step by step approach combining orthogonal measurements with increasing complexity. J Control Release. 2019;299:31-43. doi: 10.1016/j.jconrel.2019.02.030.

Chauhan I, Yasir M, Verma M, Singh AP. Nanostructured Lipid Carriers: A Groundbreaking Approach for Transdermal Drug Delivery. Adv Pharm Bull. 2020;10(2):150-165. doi: 10.34172/apb.2020.021.

Chen DH, Leu JC, Huang TC. Transport and hydrolysis of urea in a reactor-separator combining an anion-exchange membrane and immobilized urease. J Chem Technol Biotechnol. 1994;61(4):351-7. doi: 10.1002/jctb.280610411.

Clemente N, Ferrara B, Gigliotti CL, Boggio E, Capucchio MT, Biasibetti E, Schiffer D, Mellai M, Annovazzi L, Cangemi L, Muntoni E, Miglio G, Dianzani U, Battaglia L, Dianzani C. Solid Lipid Nanoparticles Carrying Temozolomide for Melanoma Treatment. Preliminary In Vitro and In Vivo Studies. Int J Mol Sci. 2018;19(2):255. doi: 10.3390/ijms19020255.

Clogston JD, Patri AK. Zeta potential measurement. Methods Mol Biol. 2011;697:63-70. doi: 10.1007/978-1-60327-198-1_6.

Das S, Chaudhury A. Recent advances in lipid nanoparticle formulations with solid matrix for oral drug delivery. Aaps Pharmscitech. 2011;12(1):62-76. doi: 10.1208/s12249-010-9563-0.

Dash S, Murthy PN, Nath L, Chowdhury P. Kinetic modeling on drug release from controlled drug delivery systems. Acta Pol Pharm. 2010;67(3):217-23.

Dibaei M, Rouini MR, Sheikholeslami B, Gholami M, Dinarvand R. The effect of surface treatment on the brain delivery of curcumin nanosuspension: in vitro and in vivo studies. Int J Nanomedicine. 2019;14:5477-5490. doi: 10.2147/IJN.S199624.

Din FU, Aman W, Ullah I, Qureshi OS, Mustapha O, Shafique S, Zeb A. Effective use of nanocarriers as drug delivery systems for the treatment of selected tumors. Int J Nanomedicine. 2017;12:7291-7309. doi: 10.2147/IJN.S146315.

Dong X. Current Strategies for Brain Drug Delivery. Theranostics. 2018;8(6):1481-1493. doi: 10.7150/thno.21254.

du Plessis-Stoman D, du Preez J, van de Venter M. Combination treatment with oxaliplatin and mangiferin causes increased apoptosis and downregulation of NFκB in cancer cell lines. Afr J Tradit Complement Altern Med. 2011;8(2):177-84. doi: 10.4314/ajtcam.v8i2.63206.

Du S, Liu H, Lei T, Xie X, Wang H, He X, Tong R, Wang Y. Mangiferin: An effective therapeutic agent against several disorders (Review). Mol Med Rep. 2018;18(6):4775-4786. doi: 10.3892/mmr.2018.9529.

Duan Y, Dhar A, Patel C, Khimani M, Neogi S, Sharma P, Siva Kumar N, Vekariya RL. A brief review on solid lipid nanoparticles: part and parcel of contemporary drug delivery systems. RSC Adv. 2020;10(45):26777-26791. doi: 10.1039/d0ra03491f.

Edwards PP, Thomas JM. Gold in a metallic divided state--from Faraday to present-day nanoscience. Angew Chem Int Ed Engl. 2007;46(29):5480-6. doi: 10.1002/anie.200700428.

Fazly Bazzaz BS, Khameneh B, Namazi N, Iranshahi M, Davoodi D, Golmohammadzadeh S. Solid lipid nanoparticles carrying Eugenia caryophyllata essential oil: the novel nanoparticulate systems with broad-spectrum antimicrobial activity. Lett Appl Microbiol. 2018;66(6):506-513. doi: 10.1111/lam.12886.

Foscolou A, Critselis E, Panagiotakos D. Olive oil consumption and human health: A narrative review. Maturitas. 2018;118:60-66. doi: 10.1016/j.maturitas.2018.10.013.

Ganguly S, Dewanjee S, Sen R, Chattopadhyay D, Ganguly S, Gaonkar R, Debnath MC. Apigenin-loaded galactose tailored PLGA nanoparticles: A possible strategy for liver targeting to treat hepatocellular carcinoma. Colloids Surf B Biointerfaces. 2021;204:111778. doi: 10.1016/j.colsurfb.2021.111778.

Gaonkar RH, Ganguly S, Dewanjee S, Sinha S, Gupta A, Ganguly S, Chattopadhyay D, Chatterjee Debnath M. Garcinol loaded vitamin E TPGS emulsified PLGA nanoparticles: preparation, physicochemical characterization, in vitro and in vivo studies. Sci Rep. 2017;7(1):530. doi: 10.1038/s41598-017-00696-6.

García D, Escalante M, Delgado R, Ubeira FM, Leiro J. Anthelminthic and antiallergic activities of Mangifera indica L. stem bark components Vimang and mangiferin. Phytother Res. 2003;17(10):1203-8. doi: 10.1002/ptr.1343.

García D, Leiro J, Delgado R, Sanmartín ML, Ubeira FM. Mangifera indica L. extract (Vimang) and mangiferin modulate mouse humoral immune responses. Phytother Res. 2003;17(10):1182-7. doi: 10.1002/ptr.1338.

Guimarães D, Cavaco-Paulo A, Nogueira E. Design of liposomes as drug delivery system for therapeutic applications. Int J Pharm. 2021;601:120571. doi: 10.1016/j.ijpharm.2021.120571.

Gupta S, Kesarla R, Chotai N, Misra A, Omri A. Systematic Approach for the Formulation and Optimization of Solid Lipid Nanoparticles of Efavirenz by High Pressure Homogenization Using Design of Experiments for Brain Targeting and Enhanced Bioavailability. Biomed Res Int. 2017;2017:5984014. doi: 10.1155/2017/5984014.

Hogarth C, Arnold K, McLauchlin A, Rannard SP, Siccardi M, McDonald TO. Evaluating the impact of systematic hydrophobic modification of model drugs on the control, stability and loading of lipid-based nanoparticles. J Mater Chem B. 2021;9(48):9874-9884. doi: 10.1039/d1tb02297k.

Hu X, Moscinski LC. Cdc2: a monopotent or pluripotent CDK? Cell Prolif. 2011;44(3):205-11. doi: 10.1111/j.1365-2184.2011.00753.x.

Imran M, Arshad MS, Butt MS, Kwon JH, Arshad MU, Sultan MT. Mangiferin: a natural miracle bioactive compound against lifestyle related disorders. Lipids Health Dis. 2017;16(1):84. doi: 10.1186/s12944-017-0449-y.

Ivanova N, Gugleva V, Dobreva M, Pehlivanov I, Stefanov S, Andonova V. Silver nanoparticles as multi-functional drug delivery systems. London, UK: IntechOpen; 2018. doi: 10.5772/intechopen.80238

Jangra A, Lukhi MM, Sulakhiya K, Baruah CC, Lahkar M. Protective effect of mangiferin against lipopolysaccharide-induced depressive and anxiety-like behaviour in mice. Eur J Pharmacol. 2014;740:337-45. doi: 10.1016/j.ejphar.2014.07.031.

Jannin V, Blas L, Chevrier S, Miolane C, Demarne F, Spitzer D. Evaluation of the digestibility of solid lipid nanoparticles of glyceryl dibehenate produced by two techniques: Ultrasonication and spray-flash evaporation. Eur J Pharm Sci. 2018;111:91-95. doi: 10.1016/j.ejps.2017.09.049.

Jimenez-Lopez C, Carpena M, Lourenço-Lopes C, Gallardo-Gomez M, Lorenzo JM, Barba FJ, Prieto MA, Simal-Gandara J. Bioactive Compounds and Quality of Extra Virgin Olive Oil. Foods. 2020;9(8):1014. doi: 10.3390/foods9081014.

Kayal S, Ramanujan RV. Doxorubicin loaded PVA coated iron oxide nanoparticles for targeted drug delivery. Mater Sci Eng C. 2010;30(3):484-90. doi: 10.1016/j.msec.2010.01.006

Kenechukwu FC, Isaac GT, Nnamani DO, Momoh MA, Attama AA. Enhanced circulation longevity and pharmacodynamics of metformin from surface-modified nanostructured lipid carriers based on solidified reverse micellar solutions. Heliyon. 2022;8(3):e09100. doi: 10.1016/j.heliyon.2022.e09100.

Khurana RK, Kaur R, Lohan S, Singh KK, Singh B. Mangiferin: a promising anticancer bioactive. Pharm Pat Anal. 2016;5(3):169-81. doi: 10.4155/ppa-2016-0003.

Kim H, Kim H, Mosaddik A, Gyawali R, Ahn KS, Cho SK. Induction of apoptosis by ethanolic extract of mango peel and comparative analysis of the chemical constitutes of mango peel and flesh. Food Chem. 2012;133(2):416-22. doi: 10.1016/j.foodchem.2012.01.053.

Kim Y, Park EJ, Kim TW, Na DH. Recent Progress in Drug Release Testing Methods of Biopolymeric Particulate System. Pharmaceutics. 2021;13(8):1313. doi: 10.3390/pharmaceutics13081313.

Kiran AR, Kumari GK, Krishnamurthy PT. Carbon nanotubes in drug delivery: Focus on anticancer therapies. J Drug Deliv Sci Technol. 2020;59:101892. doi: 10.1016/j.jddst.2020.101892.

Lee H, Mensire R, Cohen RE, Rubner MF. Strategies for hydrogen bonding based layer-by-layer assembly of poly (vinyl alcohol) with weak polyacids. Macromolecules. 2012;45(1):347-55. doi: 10.1021/ma202092w.

Lewén A, Matz P, Chan PH. Free radical pathways in CNS injury. J Neurotrauma. 2000;17(10):871-90. doi: 10.1089/neu.2000.17.871.

Lin Y, Zhou M, Tai X, Li H, Han X, Yu J. Analytical transmission electron microscopy for emerging advanced materials. Matter. 2021;4(7):2309-39. doi: 10.1016/j.matt.2021.05.005.

Luo F, Lv Q, Zhao Y, Hu G, Huang G, Zhang J, Sun C, Li X, Chen K. Quantification and purification of mangiferin from Chinese Mango (Mangifera indica L.) cultivars and its protective effect on human umbilical vein endothelial cells under H(2)O(2)-induced stress. Int J Mol Sci. 2012;13(9):11260-74. doi: 10.3390/ijms130911260.

Madane RG, Mahajan HS. Curcumin-loaded nanostructured lipid carriers (NLCs) for nasal administration: design, characterization, and in vivo study. Drug Deliv. 2016;23(4):1326-34. doi: 10.3109/10717544.2014.975382.

Makare N, Bodhankar S, Rangari V. Immunomodulatory activity of alcoholic extract of Mangifera indica L. in mice. J Ethnopharmacol. 2001;78(2-3):133-7. doi: 10.1016/s0378-8741(01)00326-9.

Mallya P, Gowda DV, Mahendran B, Bhavya MV, Jain V. Recent developments in nano micelles as drug delivery system. Int J Pharm Sci Res. 2020;11(1):176-84. doi: 10.26452/ijrps.v11i1.1804

Manzano M, Vallet-Regí M. Mesoporous silica nanoparticles for drug delivery. Adv Funct Mater. 2020;30(2):1902634. doi: 10.1002/adfm.201902634

Mazlan NA, Azman S, Ghazali NF, Yusri PZ, Idi HM, Ismail M, Sekar M. Synergistic antibacterial activity of mangiferin with antibiotics against Staphylococcus aureus. Drug Discov Today. 2019;12:14-7.

Mazur KL, Feuser PE, Valério A, Poester Cordeiro A, de Oliveira CI, Assolini JP, Pavanelli WR, Sayer C, Araújo PHH. Diethyldithiocarbamate loaded in beeswax-copaiba oil nanoparticles obtained by solventless double emulsion technique promote promastigote death in vitro. Colloids Surf B Biointerfaces. 2019;176:507-512. doi: 10.1016/j.colsurfb.2018.12.048.

Mei S, Perumal M, Battino M, Kitts DD, Xiao J, Ma H, Chen X. Mangiferin: a review of dietary sources, absorption, metabolism, bioavailability, and safety. Crit Rev Food Sci Nutr. 2021:1-19. doi: 10.1080/10408398.2021.1983767.

Mircioiu C, Voicu V, Anuta V, Tudose A, Celia C, Paolino D, Fresta M, Sandulovici R, Mircioiu I. Mathematical Modeling of Release Kinetics from Supramolecular Drug Delivery Systems. Pharmaceutics. 2019;11(3):140. doi: 10.3390/pharmaceutics11030140.

Mohammadi Ziarani G, Malmir M, Lashgari N, Badiei A. The role of hollow magnetic nanoparticles in drug delivery. RSC Adv. 2019;9(43):25094-25106. doi: 10.1039/c9ra01589b.

Mohammed A, Abdullah A. Scanning electron microscopy (SEM): A review. InProceedings of the 2018 International Conference on Hydraulics and Pneumatics—HERVEX, Băile Govora, Romania 2018:7-9.

Mura P, Maestrelli F, D'Ambrosio M, Luceri C, Cirri M. Evaluation and Comparison of Solid Lipid Nanoparticles (SLNs) and Nanostructured Lipid Carriers (NLCs) as Vectors to Develop Hydrochlorothiazide Effective and Safe Pediatric Oral Liquid Formulations. Pharmaceutics. 2021;13(4):437. doi: 10.3390/pharmaceutics13040437.

Muruganandan S, Lal J, Gupta PK. Immunotherapeutic effects of mangiferin mediated by the inhibition of oxidative stress to activated lymphocytes, neutrophils and macrophages. Toxicology. 2005;215(1-2):57-68. doi: 10.1016/j.tox.2005.06.008.

Nagarkar R, Patel J. Polyvinyl alcohol: A comprehensive study. ASPS. 2019;3(4):34-44.

Nakhaei P, Margiana R, Bokov DO, Abdelbasset WK, Jadidi Kouhbanani MA, Varma RS, Marofi F, Jarahian M, Beheshtkhoo N. Liposomes: Structure, Biomedical Applications, and Stability Parameters With Emphasis on Cholesterol. Front Bioeng Biotechnol. 2021;9:705886. doi: 10.3389/fbioe.2021.705886.

National Center for Biotechnology Information (2022). PubChem Compound Summary for CID 5281647, Mangiferin. Retrieved July 28, 2022 from https://pubchem.ncbi.nlm.nih.gov/compound/Mangiferin#section=Chemical-and-Physical-Properties.

Pal PB, Sinha K, Sil PC. Mangiferin, a natural xanthone, protects murine liver in Pb(II) induced hepatic damage and cell death via MAP kinase, NF-κB and mitochondria dependent pathways. PLoS One. 2013;8(2):e56894. doi: 10.1371/journal.pone.0056894.

Pan CW, Pan ZZ, Hu JJ, Chen WL, Zhou GY, Lin W, Jin LX, Xu CL. Mangiferin alleviates lipopolysaccharide and D-galactosamine-induced acute liver injury by activating the Nrf2 pathway and inhibiting NLRP3 inflammasome activation. Eur J Pharmacol. 2016;770:85-91. doi: 10.1016/j.ejphar.2015.12.006.

Pan LL, Wang AY, Huang YQ, Luo Y, Ling M. Mangiferin induces apoptosis by regulating Bcl-2 and Bax expression in the CNE2 nasopharyngeal carcinoma cell line. Asian Pac J Cancer Prev. 2014;15(17):7065-8. doi: 10.7314/apjcp.2014.15.17.7065.

Patel KK, Gade S, Anjum M, Singh SK, Maiti P, Agrawal AK, Singh S. Effect of penetration enhancers and amorphization on transdermal permeation flux of raloxifene-encapsulated solid lipid nanoparticles: an ex vivo study on human skin. Applied Nanoscience. 2019;9(6):1383-94. doi: 10.1007/s13204-019-01004-6.

Patra JK, Das G, Fraceto LF, Campos EVR, Rodriguez-Torres MDP, Acosta-Torres LS, Diaz-Torres LA, Grillo R, Swamy MK, Sharma S, Habtemariam S, Shin HS. Nano based drug delivery systems: recent developments and future prospects. J Nanobiotechnology. 2018;16(1):71. doi: 10.1186/s12951-018-0392-8.

Peng ZG, Yao YB, Yang J, Tang YL, Huang X. Mangiferin induces cell cycle arrest at G2/M phase through ATR-Chk1 pathway in HL-60 leukemia cells. Genet Mol Res. 2015;14(2):4989-5002. doi: 10.4238/2015.May.12.2.

Pochapski DJ, Carvalho Dos Santos C, Leite GW, Pulcinelli SH, Santilli CV. Zeta Potential and Colloidal Stability Predictions for Inorganic Nanoparticle Dispersions: Effects of Experimental Conditions and Electrokinetic Models on the Interpretation of Results. Langmuir. 2021;37(45):13379-13389. doi: 10.1021/acs.langmuir.1c02056.

Prabhu S, Jainu M, Sabitha KE, Devi CS. Cardioprotective effect of mangiferin on isoproterenol induced myocardial infarction in rats. Indian J Exp Biol. 2006;44(3):209-15.

Prabhu S, Jainu M, Sabitha KE, Devi CS. Role of mangiferin on biochemical alterations and antioxidant status in isoproterenol-induced myocardial infarction in rats. J Ethnopharmacol. 2006;107(1):126-33. doi: 10.1016/j.jep.2006.02.014.

Prabhu S, Jainu M, Sabitha KE, Shyamala Devi CS. Effect of mangiferin on mitochondrial energy production in experimentally induced myocardial infarcted rats. Vascul Pharmacol. 2006;44(6):519-25. doi: 10.1016/j.vph.2006.03.012.

Prabhu S, Narayan S, Devi CS. Mechanism of protective action of mangiferin on suppression of inflammatory response and lysosomal instability in rat model of myocardial infarction. Phytother Res. 2009;23(6):756-60. doi: 10.1002/ptr.2549.

Qamar Z, Qizilbash FF, Iqubal MK, Ali A, Narang JK, Ali J, Baboota S. Nano-Based Drug Delivery System: Recent Strategies for the Treatment of Ocular Disease and Future Perspective. Recent Pat Drug Deliv Formul. 2019;13(4):246-254. doi: 10.2174/1872211314666191224115211.

Rajendran P, Rengarajan T, Nandakumar N, Divya H, Nishigaki I. Mangiferin in cancer chemoprevention and treatment: pharmacokinetics and molecular targets. J Recept Signal Transduct Res. 2015;35(1):76-84. doi: 10.3109/10799893.2014.931431.

Rapalli VK, Kaul V, Gorantla S, Waghule T, Dubey SK, Pandey MM, Singhvi G. UV Spectrophotometric method for characterization of curcumin loaded nanostructured lipid nanocarriers in simulated conditions: Method development, in-vitro and ex-vivo applications in topical delivery. Spectrochim Acta A Mol Biomol Spectrosc. 2020;224:117392. doi: 10.1016/j.saa.2019.117392.

Rasool M, Sabina EP, Mahinda PS, Gnanaselvi B. Mangiferin, a natural polyphenol protects the hepatic damage in mice caused by CCl4 intoxication. Comp Clin Path. 2012;21(5):865-72. doi: 10.1007/s00580-011-1190-y.

Razura-Carmona FF, Pérez-Larios A, Herrera-Martínez M, Bueno-Durán AY, Sáyago-Ayerdi SG, Sánchez-Burgos JA. Zinc Oxide Nanoparticles with Mangiferin: Optical Properties, In Vitro Release Studies, and Antibacterial Activity. Revista Brasileira de Farmacognosia. 2022:1-8. doi: 10.1007/s43450-022-00268-4.

Rivera DG, Hernández I, Merino N, Luque Y, Álvarez A, Martín Y, Amador A, Nuevas L, Delgado R. Mangifera indica L. extract (Vimang) and mangiferin reduce the airway inflammation and Th2 cytokines in murine model of allergic asthma. J Pharm Pharmacol. 2011;63(10):1336-45. doi: 10.1111/j.2042-7158.2011.01328.x.

Saha S, Sadhukhan P, Sil PC. Mangiferin: A xanthonoid with multipotent anti-inflammatory potential. Biofactors. 2016;42(5):459-474. doi: 10.1002/biof.1292.

Saleh S, El-Maraghy N, Reda E, Barakat W. Modulation of diabetes and dyslipidemia in diabetic insulin-resistant rats by mangiferin: role of adiponectin and TNF-α. An Acad Bras Cienc. 2014;86(4):1935-48. doi: 10.1590/0001-3765201420140212.

Salunkhe AB, Khot VM, Thorat ND, Phadatare MR, Sathish CI, Dhawale DS, Pawar SH. Polyvinyl alcohol functionalized cobalt ferrite nanoparticles for biomedical applications. Appl Surf Sci. 2013;264:598-604. doi: 10.1016/j.apsusc.2012.10.073.

Saporito F, Sandri G, Bonferoni MC, Rossi S, Boselli C, Icaro Cornaglia A, Mannucci B, Grisoli P, Vigani B, Ferrari F. Essential oil-loaded lipid nanoparticles for wound healing. Int J Nanomedicine. 2017;13:175-186. doi: 10.2147/IJN.S152529.

Sellamuthu PS, Arulselvan P, Fakurazi S, Kandasamy M. Beneficial effects of mangiferin isolated from Salacia chinensis on biochemical and hematological parameters in rats with streptozotocin-induced diabetes. Pak J Pharm Sci. 2014;27(1):161-7.

Sellamuthu PS, Muniappan BP, Perumal SM, Kandasamy M. Antihyperglycemic effect of mangiferin in streptozotocin induced diabetic rats. J Health Sci. 2009;55(2):206-14.

Senapati S, Mahanta AK, Kumar S, Maiti P. Controlled drug delivery vehicles for cancer treatment and their performance. Signal Transduct Target Ther. 2018;3:7. doi: 10.1038/s41392-017-0004-3.

Severino P, Santana MH, Souto EB. Optimizing SLN and NLC by 2(2) full factorial design: effect of homogenization technique. Mater Sci Eng C Mater Biol Appl. 2012;32(6):1375-9. doi: 10.1016/j.msec.2012.04.017.

Shirazi AS, Varshochian R, Rezaei M, Ardakani YH, Dinarvand R. SN38 loaded nanostructured lipid carriers (NLCs); preparation and in vitro evaluations against glioblastoma. J Mater Sci Mater Med. 2021;32(7):78. doi: 10.1007/s10856-021-06538-2.

Sicurella M, Sguizzato M, Cortesi R, Huang N, Simelière F, Montesi L, Marconi P, Esposito E. Mangiferin-Loaded Smart Gels for HSV-1 Treatment. Pharmaceutics. 2021;13(9):1323. doi: 10.3390/pharmaceutics13091323.

Siddique S, Chow JC. Gold nanoparticles for drug delivery and cancer therapy. Appl. Sci.. 2020;10(11):3824. doi: 10.3390/app10113824

Sirousazar M, Kokabi M, Hassan ZM, Bahramian AR. Dehydration kinetics of polyvinyl alcohol nanocomposite hydrogels containing Na-montmorillonite nanoclay. Scientia Iranica. 2011;18(3):780-4. doi: 10.1016/j.scient.2011.06.002.

Souto EB, Doktorovova S, Zielinska A, Silva AM. Key production parameters for the development of solid lipid nanoparticles by high shear homogenization. Pharm Dev Technol. 2019;24(9):1181-1185. doi: 10.1080/10837450.2019.1647235.

Su S, Kang PM. Systemic Review of Biodegradable Nanomaterials in Nanomedicine. Nanomaterials (Basel). 2020;10(4):656. doi: 10.3390/nano10040656.

Sur S, Rathore A, Dave V, Reddy KR, Chouhan RS, Sadhu V. Recent developments in functionalized polymer nanoparticles for efficient drug delivery system. Nano-Struct & Nano-Objects. 2019;20:100397. doi: 10.1016/j.nanoso.2019.100397.

Svečnjak L, Chesson LA, Gallina A, Maia M, Martinello M, Mutinelli F, Muz MN, Nunes FM, Saucy F, Tipple BJ, Wallner K. Standard methods for Apis mellifera beeswax research. J Apic Res. 2019;58(2):1-08. doi: 10.1080/00218839.2019.1571556.

Tamjidi F, Shahedi M, Varshosaz J, Nasirpour A. Design and characterization of astaxanthin-loaded nanostructured lipid carriers. Innov Food Sci Emerg Technol. 2014;26:366-74. doi: 10.1016/j.ifset.2014.06.012.

Tayana N, Inthakusol W, Duangdee N, Chewchinda S, Pandith H, Kongkiatpaiboon S. Mangiferin content in different parts of mango tree (Mangifera indica L.) in Thailand. Warasan Songkhla Nakharin. 2019;41(3).

Telang M, Dhulap S, Mandhare A, Hirwani R. Therapeutic and cosmetic applications of mangiferin: a patent review. Expert Opin Ther Pat. 2013;23(12):1561-80. doi: 10.1517/13543776.2013.836182.

Telange DR, Sohail NK, Hemke AT, Kharkar PS, Pethe AM. Phospholipid complex-loaded self-assembled phytosomal soft nanoparticles: evidence of enhanced solubility, dissolution rate, ex vivo permeability, oral bioavailability, and antioxidant potential of mangiferin. Drug Deliv Transl Res. 2021;11(3):1056-1083. doi: 10.1007/s13346-020-00822-4.

Tenchov R, Bird R, Curtze AE, Zhou Q. Lipid Nanoparticles-From Liposomes to mRNA Vaccine Delivery, a Landscape of Research Diversity and Advancement. ACS Nano. 2021. doi: 10.1021/acsnano.1c04996.

Vieira AB, Coelho LP, Insuela DB, Carvalho VF, dos Santos MH, Silva PM, Martins MA. Mangiferin prevents guinea pig tracheal contraction via activation of the nitric oxide-cyclic GMP pathway. PLoS One. 2013 Aug 8;8(8):e71759. doi: 10.1371/journal.pone.0071759. Erratum in: PLoS One. 2013;8(9). doi: 10.1371/annotation/48d07c62-084f-4c46-b8cf-564ff59f1bd4.

Vieira R, Severino P, Nalone LA, Souto SB, Silva AM, Lucarini M, Durazzo A, Santini A, Souto EB. Sucupira Oil-Loaded Nanostructured Lipid Carriers (NLC): Lipid Screening, Factorial Design, Release Profile, and Cytotoxicity. Molecules. 2020;25(3):685. doi: 10.3390/molecules25030685.

Wang Y, Pi C, Feng X, Hou Y, Zhao L, Wei Y. The Influence of Nanoparticle Properties on Oral Bioavailability of Drugs. Int J Nanomedicine. 2020;15:6295-6310. doi: 10.2147/IJN.S257269.

Wang Z, Guo S, Wang J, Shen Y, Zhang J, Wu Q. Nrf2/HO-1 mediates the neuroprotective effect of mangiferin on early brain injury after subarachnoid hemorrhage by attenuating mitochondria-related apoptosis and neuroinflammation. Sci Rep. 2017;7(1):11883. doi: 10.1038/s41598-017-12160-6.

Wei Q, Yang Q, Wang Q, Sun C, Zhu Y, Niu Y, Yu J, Xu X. Formulation, Characterization, and Pharmacokinetic Studies of 6-Gingerol-Loaded Nanostructured Lipid Carriers. AAPS PharmSciTech. 2018;19(8):3661-3669. doi: 10.1208/s12249-018-1165-2.

Yang C, Yan H, Jiang X, Xu H, Tsao R, Zhang L. Preparation of 9*Z*-β-Carotene and 9*Z*-β-Carotene High-Loaded Nanostructured Lipid Carriers: Characterization and Storage Stability. J Agric Food Chem. 2020;68(47):13844-13853. doi: 10.1021/acs.jafc.0c02342.

Yao YB, Peng ZG, Liu ZF, Yang J, Luo J. [Effects of mangiferin on cell cycle status and CDC2/Cyclin B1 expression of HL-60 cells]. Zhong Yao Cai. 2010;33(1):81-5. Chinese.

Yoo J, Park C, Yi G, Lee D, Koo H. Active Targeting Strategies Using Biological Ligands for Nanoparticle Drug Delivery Systems. Cancers (Basel). 2019;11(5):640. doi: 10.3390/cancers11050640.

Youssef A, Dudhipala N, Majumdar S. Ciprofloxacin Loaded Nanostructured Lipid Carriers Incorporated into In-Situ Gels to Improve Management of Bacterial Endophthalmitis. Pharmaceutics. 2020;12(6):572. doi: 10.3390/pharmaceutics12060572.

Zhang Q, Kong X, Yuan H, Guan H, Li Y, Niu Y. Mangiferin Improved Palmitate-Induced-Insulin Resistance by Promoting Free Fatty Acid Metabolism in HepG2 and C2C12 Cells via PPAR*α*: Mangiferin Improved Insulin Resistance. J Diabetes Res. 2019;2019:2052675. doi: 10.1155/2019/2052675.

Zhao J, Dong T, Yu P, Wang J. Conformation and Metal Cation Binding of Zwitterionic Alanine Tripeptide in Saline Solutions by Infrared Vibrational Spectroscopy and Molecular Dynamics Simulations. J Phys Chem B. 2022;126(1):161-173. doi: 10.1021/acs.jpcb.1c10034.

Zheng MS, Lu ZY. Antiviral effect of mangiferin and isomangiferin on herpes simplex virus. Chin Med J (Engl). 1990;103(2):160-5.

Zhuang CY, Li N, Wang M, Zhang XN, Pan WS, Peng JJ, Pan YS, Tang X. Preparation and characterization of vinpocetine loaded nanostructured lipid carriers (NLC) for improved oral bioavailability. Int J Pharm. 2010;394(1-2):179-85. doi: 10.1016/j.ijpharm.2010.05.005.

Annexure

Certificate of poster presentation at International conference
and
Abstract book

ICTRHR-2022

2nd International Conference *On*

"Transforming Ripples in Healthcare Research: Obstacles, Sustenance & Cutting-edge Innovations"

Organized by School of Medical Sciences, Adamas University, Kolkata, India

Sponsored by Science and Engineering Research Board, Department of Science and Technology, Government of India

In collaboration with Central Ayurveda Research Institute (CARI), CCRAS, Ministry of Ayush, Govt. of India

Media Partner Pharmatutor

CERTIFICATE OF PRESENTATION

This is to certify that

Prof. / Dr. / Mr. / Ms. Hiranmoy Bhattacharya

from Jadavpur University

has presented a paper in ~~oral~~/poster session on the topic

Fabrication of nanostructured lipid carriers with naturally occurring compound mangiferin to enhance therapeutic efficacy

"Transforming Ripples in Healthcare Research: Obstacles, Sustenance & Cutting-edge Innovations" (ICTRHR-2022),

organized by School of Medical Sciences, Adamas University, Kolkata, India

on 10th – 11th February, 2022.

Sajal K Jha

Dr. Sajal Kumar Jha
(Associate Dean, SOMS)
Chairman, ICTRHR

PRoy

Dr. Partha Roy
(Associate Professor, SOMS)
Convener, ICTRHR

Tanmoy Guria

Dr. Tanmoy Guria
(Associate Professor, SOMS)
Co-Convener, ICTRHR

fields of medicine, pharmacy and biology and continued to play a highly significant role in the drug discovery and development process. Plant derived natural products plays a significant role in discovery of lead molecule or pharmacophores. However, even if some natural products have still been investigated in preclinical and clinical studies, the validation of their efficacy and safety as anti-tuberculosis agents is far from being reached, and therefore, according to an evidence-based approach, more high-level randomized clinical trials are urgently needed. This research article depicts the various potential plants extracts as well as plant derived phytoconstituents against the H37rv, the most persistent Strains of Mycobacterium tuberculosis and its Multidrug strains.

Keywords: Phytoconstituents, H37rv, *Mycobacterium tuberculosis*, Antimycobacterial activity, Drug resistant strains, Plants Extract

ICTRHR-PO-37

EVALUATION OF ROSMARINIC ACID FROM ROSMARINUS OFFICINALIS AS A POTENTIAL NATURAL ANTI-MYCOBACTERICIDAL MOLECULE WHICH TARGET MYCOBACTERIAL LIPOAMIDE DEHYDROGENASE

KhusbooKumaria, Romiul Islam, Nandan Sarkara*

Department of Pharmaceutical Technology, School of Medical Sciences, Adamas University, Kolkata-700126, West Bengal, India

***Email:** nandan1.sarkar@adamasuniversity.ac.in

Abstract: Tuberculosis (TB) is one of the dreadful infectious diseases. After almost 30-40 years of stagnant drug development, the past few years has perceived the need of promising anti-TB drugs due to the complicated situation of multi-drug resistant and extensively-drug resistant strains of the organism. Antimycobacterial activity of the high-altitude medicinal plants *Rosmarinus officinalis* (*R. officinalis*) was evaluated using colorimetric redox indicator (CRI) assay and the probable targets were identified by molecular docking study. The ethyl acetate fraction of *R. officinalis* showed maximum antimycobacterial activity with MIC 125 μg/ml against all the tested strains of M. tuberculosis (H37Rv and MDR). Based on bioassay guided fractionation and isolation, the marker compound rosmarinic acid (RA) was identified as potent molecules that exhibited the MIC in the range of 15-32 μg/ml against both H37Rv and MDR strains of M. tuberculosis. With the docking analysis among 10 targets, Rv2623 and lipoamide dehydrogenase were predicted as Mtb targets of RA; however, MD simulation studies on these complexes indicated that Mtb lipoamide dehydrogenase is the preferred and probable target for RA. This is the first report of Rosmarinic acid as an active anti-mycobactericidal agent which further established through molecular docking and stimulation studies.

Keywords:*Rosmarinus officinalis*, Rosmarinic acid, Antimycobacterial activity, Molecular docking, Molecular dynamics simulation, Lipoamide dehydrogenase

ICTRHR-PO-38

FABRICATION OF NANOSTRUCTURED LIPID CARRIERS WITH NATURALLY OCCURRING COMPOUND MANGIFERIN TO ENHANCE THERAPEUTIC EFFICACY

Hiranmoy Bhattacharya*, Pratik Chakraborty, SaikatDewanjee

Advanced Pharmacognosy Research Laboratory, Department of Pharmaceutical Technology, Jadavpur University, Kolkata 700032, India

***Email:**hiranmoy270@gmail.com

Abstract: Mangiferin (2-β-D-glucopyranosyl-1,3,6,7-tetrahydroxy-9H-xanthen-9-one) is a naturally occurring polyphenol, which exhibits several therapeutic attributes, such as anti-diabetic, anti-hyperlipidemic, antioxidant, immunomodulatory, and anti-allergic activities. However, this drug showed very poor bioavailability. Thus, it has been aimed to formulate mangiferin-loaded nanostructured lipid carriers (MNLC) to enhance the bioavailability of mangiferin. MNLC were prepared by common solvent diffusion in an aqueous system using solid and liquid lipids, common solvent system, and surfactant. Distinctive peaks of each of the components (lipids, surfactant, and

drug) are present in the FTIR spectra of the formulation, which proves there is no chemical modification of the components in formulation. The formulation showed a mean particle size of 310.87 ± 22.01 nm with the polydispersity index of 0.175 and zeta potential of -10.5 mV. The entrapment efficiency was found to be 75.2% with a mean drug loading percentage of 3.79% in the formulation, which was calculated by plotting the standard curve. MNLC exhibited initial burst release of mangiferin followed by a slow and sustained drug release up to 8 days. MNLC exhibited initial burst release of drug followed by a slow and sustained drug release for about 8 days with cumulative release of 88% at the end of 8 days. In addition, MNLC displayed enhanced cellular internalization of mangiferin, which may strengthen the biological activity of the formulation.

Keywords: Bioavailability; Cellular internalization; Mangiferin; Nanostructured lipid carriers.

ICTRHR-PO-39

CHALLENGES AND CLINICAL TRANSLATION OF NANOPARTICLES IN LUNG CANCER THERAPY

Bhavna Yadav, Rahul Pratap Singh*

Department of Pharmacy, School of Medical and Allied Sciences, G.D. Goenka University, Gurugram-122103, India.

Email: 200100602011.bhavna@gdgu.org

Abstract: Lung cancer is divergent by nature and develops quietly in the lungs and is known to have second leading cause of cancer in the world, reporting ~14% of freshly diagnosed cases every year with highest mortality rates. In India, lung cancer constitutes 6.9% of all new cancer cases and 9.3% of all cancer related deaths in both sexes; it is the commonest cancer and cause of cancer related mortality in men. Traditional cancer therapies have inherent limitations, prompting the formulation and deployment of diverse nanotechnologies for more effective and safer cancer treatment, referred to as nanomedicine. However,the complexities and heterogeneity of tumor biology, an incomplete understanding of nano–bio interactions, and the challenges of chemistry, manufacturing, and controls required for clinical translation and commercialization are the main obstacles to nanomedicine becoming a new paradigm in cancer therapy. It highlights that the therapeutic approaches are hampered by a translational gap between basic scientists, clinicians and pharma industry due to suboptimal animal models and difficulties in scale-up production of nanoagents. Henceforth it is needed to overcome these forbetter clinical outcomes in lung cancer therapy.

Keywords: Lung cancer, Nanomedicines, Clinical studies, Nanoparticles, Animal model

ICTRHR-PO-40

***CASSIA FISTULA* SEED GUM-G-POLY (SODIUM ACRYLATE) COPOLYMER: SYNTHESIS, CHARACTERIZATIONS AND FABRICATION INTO SUSTAINED RELEASE GASTRIC-MUCOSA-ADHESIVE TABLET OF ACECLOFENAC**

Abhijit Changder[1*], Riyasree Paul[2], Gouranga Nandi[3], Lakshmi Kanta Ghosh[1]

[1] Department of Pharmaceutical Technology, Jadavpur University, Jadavpur, Kolkata–700032, India; [2]Department of Pharmaceutical Technology, Brainware University, 398, Ramkrishnapur Road, Barasat, Kolkata – 700125, India; [3]Division of Pharmaceutics, Department of Pharmaceutical Technology, University of North Bengal, Raja Rammohunpur, Dist. Darjeeling, West Bengal, Pin – 734013, India

***Email:** changder.abhijit@gmail.com

Abstract: In this study, *Cassia fistula* seed gum (CFSG) was grafted with poly (sodium acrylate) to develop a natural polysaccharide based mucoadhesive sustained-release copolymer. Mucoadhesive sustained-release tablets were prepared with the copolymer and a model drug aceclofenac by wet granulation technique and evaluated. Compatibility between drug and excipients was checked by DSC, FTIR and XRD analysis. The tablets showed excellent mucoadhesion comparable to synthetic mucoadhesive-polymer carbopol with mucoadhesion time > 10 h. The tablet composed of the copolymer with highest percentage 1190% grafting showed a significantly higher T90% of 14.7 h, which ratifies the sustained-release capacity of the copolymer.

Keywords:*Cassia fistula*, Sodium acrylate, Sustained release.